POLITECNICO DI MILANO
Laurea Magistrale in Ingegneria Meccanica
School of industrial and information Engineering

A new type of Variable Stiffness Actuator using a Continuously Variable Transmission: mechanical and control design

Relatore: Prof. Giuseppe Bucca
Correlatore: Ing. Alessio Prini

Thesis of:
Nader Riman
matricola 895619

Academic Year 2019-2020

Abstract

In this thesis, we design and control a new type of variable stiffness actuator, an actuator that has a compliant element with the ability to change it's stiffness thanks to a continuously variable transmission. We will show that by adjusting the intrinsic stiffness, through applying the optimal control theory to get a task-specific trajectory and stiffness profile, it will result in the best performance or highest efficiency the system can reach depending on the required task. In this thesis, we will be applying an explosive movement task to show the advantages in reaching higher velocities and higher availability of power to use that a variable stiffness actuator can provide over other classes of actuators such as series elastic actuator and the classical rigid actuator. An extensive comparison between the VSA and SEA will be done to highlight how changing a stiffness can highly affect a system's performance. The control strategy adopted consits of a time-varying finite horizon LQR that accounts for the non-linearities of the system and a low level torque control which relies on position control thanks to the proportional relation between deflection and force of the spring. Unfortunately, experimental results are missing due to an unexpected tragedy that hit the world (CoVid-19) and prevented physical work on this thesis.

Acknowledgements

My deepest gratitude goes to Ing. Alessio Prini for his continuous support during this journey, I have learned a lot from him during this project and I deeply appreciate the technical experience in design and control I have gained from working under his supervision. Also, I would like to thank Prof. Giuseppe Bucca for his follow-up and offering help and equipment in critical situations. I would also like to express my gratitude to the CNR team, Dr. Matteo Malosio for providing this opportunity and Ing. Tito Dinon for his insight in mechanical design.

And most importantly, I would like to thank my family and friends for all the much-needed emotional support that helped me stay motivated throughout those 2 years and especially my parents for their excellent support for me in the most vulnerable situations.

Contents

Chapter 1

Introduction

Since the 60s and 70s, the first generation of robots have been used intensively in the industrial sector to carry out different tasks. In modern production plants, particularly in large assembly lines, robots have replaced people in carrying out tasks that are generally really heavy or repetitive, such as material handling of heavy parts in hazardous environments, painting tasks in car assembly lines, welding etc. This first generation consists of robots able to perform sequences of operations in well defined environments and regardless of the presence of humans in the working area. For this reason a lot of safety devices and procedures are used in order to avoid the coexistence of humans and robots.

In modern years we are witnessing a paradigm shift in robotics from a hierarchical one, where a robot is not able to react to the external environment perturbation, to a reactive paradigm, where the robot action changes based on the external output in terms of force, vision or other external measurements.

This change has made it possible to move onto a new generation of robots able to react, on the basis of the control strategy chosen, to disturbances in the external environment, including the human presence. This new generation of robots comprises the so called collaborative robot (cobot), a robot designed to interact with humans in a shared space or to work safely in close proximity.

The ability to react to changeable outdoor environments and to share the work space with humans, without posing a danger to their safety, is an indispensable feature also for other types of robots such as humanoids or service robots that today appear on the market and in the world of research. A well-known example is the one of the service robots produced by iRobot,

with their most famous product Roomba. Service robots are a perfect support for the medicinal services industry thanks to their precision, accuracy, speed, flexibility and ability to work together with people. These robots are presently being utilized by research facilities, in medical procedures, rehabilitation, support and improve the well being and lives of people around us [1]. Revolutionary advancements can be made through the integration of this innovative technology, which is significantly improving the recovery and quality of life for patients [1].

Robotics is a field of engineering that involves several tracks of engineering most importantly mechanical engineering and electronics, where it is responsible of the hardware part (design and construction) and software part (control and sensory feedback) that produces machines, with the goal to substitute (or replicate) human actions, the end product is what we call a Robot [2]. Industrial robots are the first type of robots[3] and in the past they were mainly used for basic classical handling, assembly and welding tasks to a wide range of production applications such as quality control, robot shaping, cutting, friction stir welding, folding and machining [4]. However, the need for the coexistence of robots and people in the physical area, by sharing the same workspace and actually interacting in a physical way, introduces the key issue of guaranteeing of the well being to the person and the robot's safety. As far as industrial robots for the most part they require secluding the workspace of the manipulators of that of the person by a door or a barrier. Then again, an expanding interest is emerging in domestic and industrial service robots, and in some situations even unavoidable physical collaboration. Along these lines, a subsequent fundamental prerequisite is to ensure safety for human users in normal activity mode just as in faulty modes [5]. Humanoids are robots, nowadays relegated only to research areas, designed to resemble humans, both functionally and aesthetically. This type of robot can be thought of as a lab robot through which it is also possible to face new technological challenges. The research and use of collaborative service robots and humanoids have shown some evident technological limits of the mechanical structures that today characterize modern robots. The robots are in fact generally made up of a chain that can be closed or open with rigid links moved by actuators placed at the joints. These actutors are generally pneumatic, hydraulic or much more frequently electric [6], chosen for their low cost and ease of use. The need for interaction with the external environment is usually addressed by sensing the robot more frequently through the use of force sensors or vision systems and a suitable control system. The adoption of this type of structure has shown all its limitations over the years in comparison with the animal exoskeletal system. The human ex-

oskeletal system in union with the central nervous system allows it to adapt to a multitude of external environments but also to express performances that do not seem attainable today with the classic mechatronic systems developed. Consider, for example, the ability of a modern footballer to kick a ball at hundreds of km/h towards the goal, and after a few seconds to collide safely with an opposing footballer; this enormous versatility in carrying out the tasks is essentially linked to the elasticity of our exoskeletal system and to the ability of the nervous system to properly exploit this elasticity. For this reason, over the years there has been a growing interest in robotic systems that somehow include elasticity in their structure, and at the same time control strategies have been developed that can properly exploit the mechanical characteristics of the robot to better perform different tasks. In an initial phase, robotic research tried to delegate this elastic property exclusively to appropriate control strategies, using particularly ready force sensors and actuators. Even this strategy today shows limitations, due for example to the impossibility of storing and releasing energy efficiently. The scientific community therefore has started to create robotic structures characterized by their intrinsic elasticity. Nowadays elasticity can be integrated either through flexible links or through joints suitably designed to include an elastic element. Elastic couplings in robotics are today divided into two broad categories, the Serial Elastic Actuator (SEA) or the Variable Stiffness Actuator (VSA). The latter can modify, generally through mechanical reconfiguration, their elastic characteristics. This device, integrated into a robot and assisted by appropriate control strategies, allows the achievement of performances that approach those of the human musculoskeletal system and are certainly part of the enabling technologies for the current and future generation of robots. To date, this type of actuator is exclusively present in the research field but does not find real uses in the industrial world, despite the advantages indicated above. This is still due to the absence of a prototype that provides the desired performance levels, the excessive cost and the non-negligible weight for this type of systems in general.

Different research groups around the world are therefore trying to find solutions to these application problems. This thesis aims to analyze some of the problems affecting the actuators present in the literature today and to investigate in particular a solution already proposed at a theoretical level by a Dutch research group which, however, does not find experimental references at the moment. This study presents a prototype for a variable stiffness actuator using a continuously variable transmission (CVT). In order to reach a variable stiffness, different factors can be changed, and one of them is the gear ratio between the output link and the compliant element, where

a high gear ratio results in high stiffness and vice versa. The scope of this thesis is to use a new type of bike CVT (figure1.1), and validating this prototype consists of demonstrating the improvements of a VSA over a serial elastic actuator by applying, in the presented case, an explosive movement task which requires reaching high velocities in a small period. The data to be collected will provide information about the efficiency and performance gained in result of this device.

Figure 1.1: Sectioned CVT transmission.[7]

These kinds of robotic applications require a new kind of enabling technologies, the robots are mainly built from a series of actuators and links properly joined together. Actuators are key enabling components for motion generation and control with properties that greatly impact the overall performance of any mechanical systems. In general in robot construction the interest is more on electric actuators,due to their high precision for position control and great control flexibility [8]. The lack of suitable actuators has hindered the development of high-performance machines with capacities equivalent to people, particularly as for movement, safety and efficiency of animal beings and humans. The functional and neuro-mechanical control performances of natural muscle far surpasses that of mechanical instruments, with a key contrast being the adaptable compliance or variable stiffness found in organic systems; this is very different from the performance of traditional stiff electrical drives used in industrial robotics, which require accurate reference-trajectory tracking [9]. However, in robotics applications it is often desired to have varying characteristics of the actuator when it comes to speed and force which are related through the stiffness of the actuator, and also in achieving human-like locomotion therefore having a variable stiffness actuator(VSA); an actuator that can inherently change the mechanical compliance of the system it is in, has positive outcomes in terms of energy efficiency,

robustness against disturbances and similarity with human motions, we obtain an actuator with different combinations of speeds, torques and stiffness. The graph in figure(1.2) shows how the three are related. This device in-

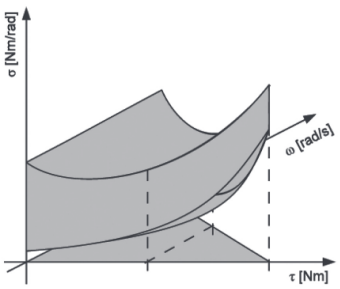

Figure 1.2: 3D graph showing the working volume of a VSA with the output stiffness(z-axis) , output velocity (y-axis) and output torque(x-axis)[10]

creases performance and efficiency by optimizing the energy storage/release of the spring and the stiffness.

In this work a detailed analysis of SEA and VSA actuators will be done, focusing in particular on the CVT-VSA actuator. As already demonstrated earlier, there are many features that make the use of an elastic actuation in the construction of robots advantageous, and there are many applications that can take advantage of these features. In order to demonstrate these advantages of CVT-VSA we will focus on a particular application, i.e. the launch of a basketball at the maximum distance. This simple application allows to show how an elastic actuation can be exploited to improve the performance of a robot during explosive movements.

In order to achieve this goal the work has been divided as follows. In Chapter 2 the state of art will be introduced in order to make the reader aware of the solutions currently present in the literature. In Chapter 3 it will be shown how it is possible to model this type of actuator from the mechanical point of view. This phase is useful in order to correctly design all the components that must then be used in the construction of the actuator, considering the particular task chosen. In Chapter 4 the complete mechanical design of CVT-VSA actuator will be shown with a brief introduction to all the elements that make up the test setup. In chapter 4 a more refined model will be shown. This phase will deviate from the work shown in Chapter 2 for the choice of real parameters to be used in modeling, and for the design of control strategies that best suit the task in question. Finally, in Chapter 5, a comparison will be made in terms of performance between the

three configurations introduced here (rigid actuator, SEA, VSA) in order to show the quality of the solutions adopted.

Chapter 2

State of the art

2.1 Collaborative robots and safety issues

Robots have been used in industry for more than 80 years and their job is to replicate or substitute humans in a faster, safer and more efficient way. But humans have been always secluded from being present in the same workspace with a working robot due to safety issues[11]. Advancements in technologies are continuously working on increasing the collaboration between the two. Collaborative robots are the type of robot coexisting and physically cooperating with people, being capable of natural motions and much closer to human performance than today's robots. As the first rule in Robotics by Isaac Asimov stated "a robot may not injure a human being or, through inaction, allow a human being to come to harm" [12] .This sentence summarises that safety in robotics is the most important aspect. This requires that robots with similar size and mass as humans also have comparable power, strength, velocity and interaction compliance. However, this goal cannot be easily reached with today's technology, where robots are very rigid for the sake of position precision [10]. When robots operate in a dynamic environment, unexpected collision between robot and the environment are likely to occur. It is important that during these collisions, both the robot and the object it is colliding with suffer as little damage as possible. Especially when the collision happens with a human, in this case the impact could lead to severe injury or fatal wound for the human. Standard industrial robot systems, due to their inertia, structure and process forces, can pose serious hazards to humans [13]. Interest in robots allowing physical interaction is highly increasing and, unlike their classical counterparts, they take into account for the hardware design, meaning the robot cannot simply rely on computed trajectories, extra precautions are required.

Figure 2.1: Robot human interaction. [14]

In order for the robot to be dynamically aware of it's environment, joints with position control are not enough, the force on the joints has to be dealt with by the robot also, for example a joint that's trying to reach a reference point by position control will try to reach that point without any considerations. However, in a case where the joint is stuck with an obstacle during the transition to the reference point, with position control, it will try it's full power to reach this point disregarding the stresses applied on it's system's body/joint, but what if we have feedback on the force too, it would prevent it from trying to overcome the obstacle to a point where it harms itself or the obstacle (which could be a human) blocking the way. To tackle this issue, a control approach is widely used to change the impedance of the system using control.

2.1.1 Variable Impedance by Control

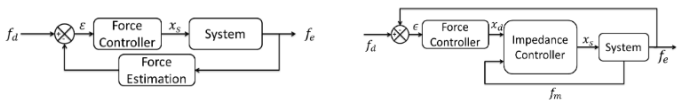

Figure 2.2: Force control vs Impedance control schematic [15]

Research on robot force control has boomed in the past thirty years. Such high interest is motivated by the desire of providing robotic systems with better sensory capabilities. Robots using force, touch, distance, and visual feedback are expected to autonomously operate in unstructured environments [16] . Force control is conveniently used with position control as a hybrid Force/Position feedback [17], adding extra feedback for robots that rely heavily on force feedback be it in Industrial applications (welding...) or

for interaction with humans. Impedance by control is a control approach that imposes a dynamic behavior between end-effector and environment. It is probably the most common control strategy to physically interact with robots. It took high academic attention after the detailed works of Hogan (1985) on Impedance Control and its implementation [18], where it imposes a desired physical behavior with respect to external forces on the robot and facilitates stable robot interactions with the environment by replicating soft and passive contacts. For example, the robot is controlled to behave like a second order mass spring damper system. Consequently, impedance control allows us to realize compliance of the robot by means of control. Force control and impedance control are similar yet different: they both use force feedback from a sensor but on the other hand, the force control has the desired force as output and impedance control aims to change the dynamics of the system to a desired impedance during contact [3]. Interaction with a well-designed impedance-controlled robot is very robust and intuitive, disturbance response is also added to the commanded trajectory. A major advantage of impedance control is that contact discontinuities do not create such stability problems in these systems. Movements are mostly realized with stiff actuation in combination with rigid high geared transmission mechanisms [19]. It is used in many applications ranging from manipulators performing tasks while in contact with the environment, humanoid robots and a wide range of human machine interfaces ranging from simple desktop haptic devices to rehabilitation robots and full body exoskeleton systems [20].

However, a force sensor is required for impedance control. Such sensors are known to be expensive in automation applications where high precision is required. In order to track rapidly the force trajectories , the controller bandwidth has to be high. It can be increased by increasing the gains, however, the gains cannot be increased beyond some limits, as the system will become violently unstable [21]. Some problems may arise affecting the stability of the robot that relies on the feedback from the force sensor, using a low pass filter to remove the high frequency noise decreases the bandwidth. Therefore, the cut-off frequency should be chosen carefully. By using the force sensor there's a trade-off between stability of the system and the response time.[22]

So in operations that are force controlled, the sensor dynamics have to be taken into account in the design of the controller, due to them being of the same order of magnitude of the whole system's dynamics. The dynamics of the sensor are not only influenced by the sensor itself but also by the system's dynamics, (higher loads carried at the sensor reduce its bandwidth)[23] and

filtering.
Albeit of its large usage in modern robots, the variable impedance control lacks of an appropriate storage mechanism (such as a spring), much of the energy is wasted and has to be continuously injected by active actuation. The energy wasted is not negligible and can have high impact on the design of mobile robots: for example a more energy efficient robot requires a small battery which account for a part of the robot's weight. And sometimes if we have multiple robots in a plant, this difference in energy consumption makes a big difference on a large scale.
In the next sections, we will talk about alternatives to impedance control where we can take advantage of the energy that is lost by adding a compliant element, between actuator and load, that can be exploited to store energy and use it to increase the efficiency of the system and/or performance depending on the application.

2.2 Serial Elastic Actuators

Traditional actuators are characterized by a very high stiffness between actuator and load, which makes it a perfect candidate for a precise position control and stability but makes it a hazard in collaborative applications due to the very high stiffness.

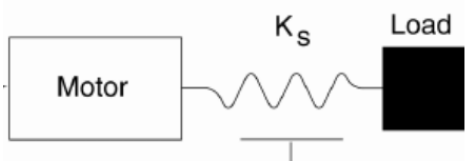

Figure 2.3: Serial Elastic Actuator

From the analysis of the problem related to stiff actuation, Pratt (1984) broke the tradition of making the interface between the actuator and the load as stiff as possible realizing many advantages could be exploited from it. This new type of actuator, back then, was called Series elastic actuator which consists of a spring between motor and load, therefore reducing the high stiffness between the two. It presents several advantages such as, greater shock tolerance, lower reflected inertia, more accurate and stable force control, less inadvertent damage to the environment, and the capacity for energy storage.[24]
Torque control in traditional actuators is a complex task, but since the introduction of a spring between the motor and the load, it is proportional

to the relative difference between motor position and load position, so the torque control transforms into position control. Moreover it is important to consider the energy storage in the spring which can help increase the efficiency of the system [25]. Despite the advantages deriving from the use of SEA actuators, the introduction of an elastic element can lead to disadvantages mainly related to positioning errors and limited stiffness. For this reason non-linear SEA can offer some solutions to the linear SEA problems. The main characteristic in linear SEA models is the spring stiffness, which is relatively proportional to the force bandwidth, so the higher the stiffness the higher the force bandwidth. But there's a trade off between high bandwidth and impedance, the more we increase the stiffness, the impedance also increases. On the other hand, for the same force bandwidth of a linear SEA, a non-Linear SEA (non-constant stiffness) has a lower impedance for example in the stiffening spring used in [26]. Non-Linear SEA such as the HypoSEA which stretches the linear spring in a non-linear way resulting in a high range of force control levels (4 orders of magnitude difference) from torques less than 0.02 N.m, because the actuator starts with a low stiffness which allows to obtain high resolution torques, to 120 Nm, because the final stiffness is high therefore allowing high torques to be transmitted, [27] and other actuators such as [28] where the actuator has a high stiffness that is used for high precision position control until a high impact force is applied on it where the force value exceeds a pre-determined threshold, at that point the actuator has a low stiffness that is suitable for shock absorption. In this case of non-linear SEA it was taken advantage of the high position precision of rigid actuators and the shock absorption of a low stiffness device.[28]
Another way to exploit a compliant element and benefit from variation of stiffness will be discussed in the next section about the prosperous Variable stiffness actuators and their different designs and ways to manipulate the stiffness of a system.

2.3 Variable Stiffness Actuators

Variable stiffness actuators (VSA) are a class of actuators that posses multiple compliant elements and internal separately actuated degrees of freedom, that allow the capability of changing their apparent output stiffness independently from the actuator output position. The introduction of a mechanical compliance introduces intrinsic, passive oscillatory behavior to the system, but rather than trying to minimize this effect, the question arises if it can be exploited for the actuation of periodic motions . the papers [29][30] allow us to observe controlling a VSA to match their natural oscillations with a cyclic

motion pattern, embodying a desired behavior of the system while minimizing the energy input to the system. Variable stiffness actuators are serial elastic actuators with the ability to change stiffness. In order to change the stiffness,It can be done in three different ways shown in the (fig.2.4).

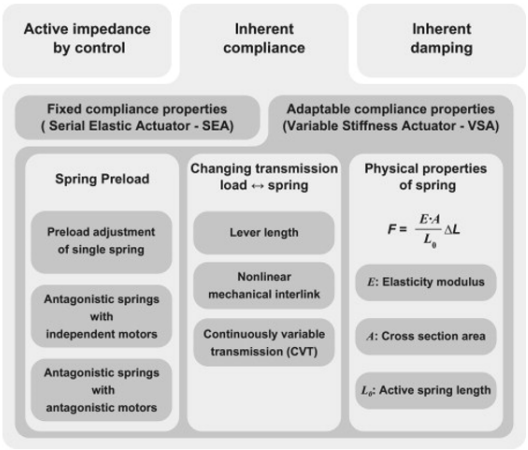

Figure 2.4: Different ways to change the stiffness [9]

In order to change the stiffness, the system is constituted of at least 2 motors (one for the actuator and one to change the stiffness).

2.3.1 Spring Preload

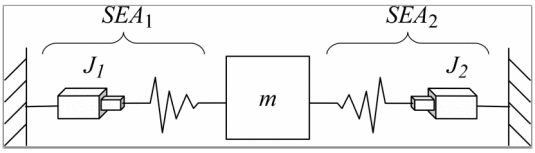

Figure 2.5: The LinArm device with the two pre-loaded non-linear springs in opposite direction to each other. [31]

In the Spring Preload category, the stiffness is adjusted by changing the pretension or preload on the spring. Compared to the no load category, the spring force is parallel to the spring displacement, hence, to change the stiffness, energy has to be stored in the springs and may not be retrievable. To overcome this a second spring with negative stiffness can be added, usually resulting in a large passive angular deflection. One application is the LINarm device for upper limb rehabilitation [31] where it uses two non-linear springs(two linear springs in triangular form from each side, resulting in one

non-linear spring, 4 linear springs used in total) in parallel in order to obtain a VSA, and this setup can only be done with nonlinear springs [9]. The two springs have a resultant stiffness and equilibrium position controlled by two motors working together. When the motors rotate in the same direction the equilibrium position changes and when they rotate in opposite directions the stiffness changes because of the non linearity.

2.3.2 Changing ratio between load and spring

The stiffness is adapted by changing the transmission ratio between the output link and the spring element for example the mVSA-UT, a miniaturized VSA, that can change its output stiffness independently of its output position through varying the transmission ratio between the internal mechanical springs and the actuator output . As this design does not pre-load the spring, theoretically at equilibrium, no energy is required to change the stiffness since the force on the spring is orthogonal to the spring displacement. In practice, friction has to be overcome and when the joint is not at the equilibrium position energy is still needed to adjust the stiffness. Nonetheless, energy consumption can be reduced. Another way to change the ratio is the lever arm mechanism with variable pivot point used in the CompAct-VSA.[32]

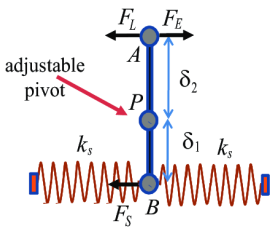

Figure 2.6: Schematic of the lever arm mechanism with variable pivot point. [32]

This class can be further divided into the following sub-classes:

- Lever length: the stiffness is adapted by controlling the configuration of a lever mechanism.
- Nonlinear mechanical link: the stiffness is adapted by controlling the properties of a nonlinear mechanical link.
- Continuously variable transmission: the stiffness is adapted by controlling the transmission ratio of a continuously variable transmission.

2.3.3 Changing physical properties of a spring

Unlike the previous concepts, structure control modulates the effective physical structure of a spring to achieve variations in stiffness. To understand the basic concept, consider the basic elasticity law:

$$F = \frac{E \times A \times \Delta L}{L_0} = K\Delta L$$

F is the force, E the material modulus, A the cross-sectional area, L the effective beam length, and ΔL is the extension. In this representation, $\frac{EA}{L}$ represents the stiffness K. To control the structural stiffness, any of the three parameters in this equation can be manipulated. E is a material property, which cannot be controlled by a structural change, but for some materials, it can be changed e.g. by changing the temperature[33]. Unfortunately, these changes are very slow for such applications[9]. Another technique [34] is to alter the cross section by having a beam with multiple sheets: the elasticity of the beam is changed by applying a vacuum force to change the total cross section of the beam. The stiffness can vary in a range of the number of sheets squared.Other papers realized this using electrostatic force and pneumatic force[35]. Other ways to change the stiffness by changing the active spring length, by The Mechanical Impedance Adjuster [36], which contains a leaf spring, connected to the joint by a wire and a pulley. The active length of the spring is changed by a slider,the spring is held close to the structure thanks to the roller on the slider. a feed screw is rotated by a motor, moving the slider and therefore changing the stiffness.
In achieving energy efficient actuation with variable stiffness actuators, an experiment was done by [37] comparing a SEA and a VSA by measuring the final velocity of a hammer before impact. The results show that the SEA has reached velocity around 300% higher than the motor's maximum velocity (due to taking advantage of the spring's stored energy), then the VSA has reached a maximum velocity 30% higher than the one reached by the SEA. Another paper studies the energy consumption of another concept of compliant actuators that exploits the dynamics by matching the compliance of the actuator with the compliance of the system [32] . The desired motion should be periodic in nature and the variable stiffness actuator should be efficient in changing the apparent output stiffness. The first condition implies that it is sensible to temporarily stored energy, because periodic motions have an energy conserving property. The second condition ensures that using a variable stiffness actuator is a sensible solution. Applications of VSA are

consequently found where robots must physically interact with an unknown and dynamic environment for example the MACCEPA actuator was used for Jumping robot[38], bipedal walking robot [39][40] therefore, the control body actuator system must have abilities like :

- shock absorbing
- stiffness variation with constant load
- stiffness variation at constant position
- cyclic movements
- explosive movements

This thesis is inspired by the concept E2V2 introduced by Stramigioli [41] in his paper "A concept for a new Energy Efficient Actuator" that concentrates on the negative power produced by the Infinitely Variable Transmission combined with an elastic element, the concept is about introducing a Continuously variable transmission which provides a smooth & continuous change of the gear ratio between input and output and thus can be used to change the apparent stiffness of the elastic element introduced independently of the equilibrium position.

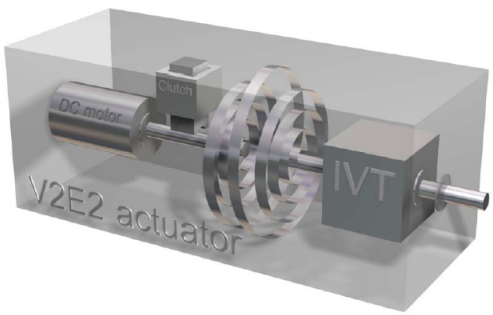

Figure 2.7: E2V2 Concept [41]

2.4 Continuously Variable Transmission

In the course of the most recent two decades, noteworthy research exertion has been coordinated towards creating vehicle transmissions that reduce the energy consumption of cars. This effort has been an immediate outcome of the developing ecological concern forcing the orders of exhaust emissions and increased vehicle efficiency on current vehicle producers and clients. A

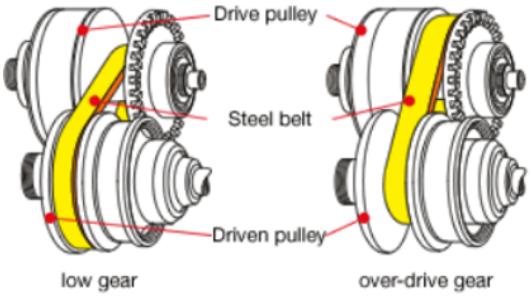

Figure 2.8: Variable Diameter Pulley CVT [42]

continuously variable transmission (CVT) offers a continuum of gear ratios between desired limits, which subsequently improves the efficiency and dynamic execution of a vehicle by better coordinating the motor working conditions to the variable driving scenarios[43] .

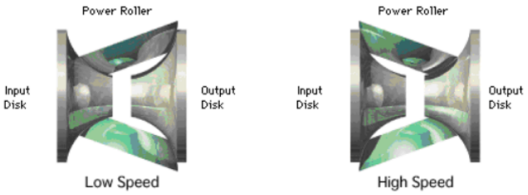

Figure 2.9: Toroidal CVT at limit positions [44]

A CVT is a growing car transmission innovation that offers a continuum of gear proportions among high and low limits with less moving parts. Thus, this improves the mileage and increasing performance of a vehicle by permitting better coordinating of the motor working conditions to the variable driving situations[43][45]. Today, CVTs are forcefully rivaling the usual transmissions and car companies are as of now enthused about using the different points of interest of a CVT in a generation vehicle. A continuously variable transmission is likewise a promising power-train innovation for future hybrid vehicles. So as to accomplish lower emissions and better performance, it is important to catch and comprehend the itemized dynamic connections in a CVT framework so productive controllers could be intended to defeat the current losses and improve the mileage of a vehicle. There are numerous sorts of CVTs, each having their very own attributes for instance Variable-diameter pulleys (VDP) or Reeves drives, Toroidal or roller-based continuously variable transmission (CVT) and Magnetic CVTs [45][46].

Be that as it may, belt and chain types are the most normally utilized CVTs, among all, in car applications.

Figure 2.10: Nuvinci CVT [47]

The NuVinci CVP is a compact and high torque-density unit that uses planetary spheres to offer continuously variable speed ratio control in wide-ranging applications. When coupled with an advanced, yet economical control system to vary the speed ratio for optimal power-train operation, the system shows benefits in overall vehicle performance.

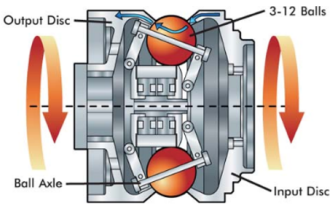

Figure 2.11: a simplified cross section of the NuVinci CVP. A bank of balls (planets) is placed in a circular array around a central idler and in contact with separate input and output discs (or traction rings).[47]

Power comes through the input disc and is transmitted to the balls, then to the output disc via traction at the rolling contact interface between the balls and discs.

The speed ratio is defined by the tilt angle of the ball axis, which changes the ratio of r_i to r_o, and thus the speed ratio . The result is the ability to sweep the transmission through the entire ratio range smoothly, while in motion or stopped. Choosing the right gear ratio at the right moment in accordance with the torque input from the motor can be seen as an optimization problem in order to obtain the desired control inputs.

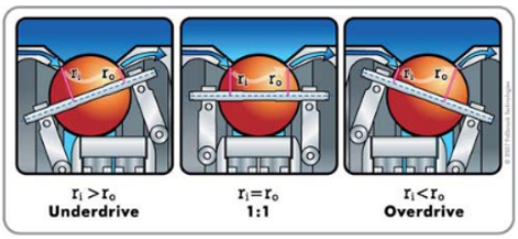

Figure 2.12: presents the system kinematics, where r_i is the contact radius of the input contact, and r_o is the contact radius at the output contact.[47]

Chapter 3

System Dynamic model and Trajectory optimization

In order to better investigate the mechanisms of operation of the VSA actuators and to better interpret the results obtained from subsequent experimental tests, it is considered necessary to proceed by modeling the system.

As already mentioned, the objective of this work is the definition of an experimental setup based on a new type of VSA actuator. To proceed with the system sizing and commercial components identification, it must first identify an application task. In this work we will focus on the ability of VSAs to store and release energy. The store and release energy mechanism is the same that is used by the muscles during the throwing of objects, as in baseball the pitcher who pulls the ball towards the catcher.

Precisely for this reason we will initially focus on a basketball ball throwing task. The goal will be to make the throw as efficient as possible or in more basic terms to throw the ball as far as possible.

As the commercial components to be used and therefore their real performances are not yet available, an ideal system will now be modeled hereafter in this chapter, in which all the components do not show friction, efficiency or delay. This ideal model is also useful for checking the suitability of the tools to be used. In order to identify the quantities involved and proceed with the sizing in addition to the model, it is also useful to consider the trajectory that will be performed by the system. Starting from a careful analysis of the state of the art [8] [48] it was verified how it is necessary to use an optimization algorithm to identify the ideal trajectory for the launch. This algorithm will be identified and validated in this chapter once the motor power is identified.

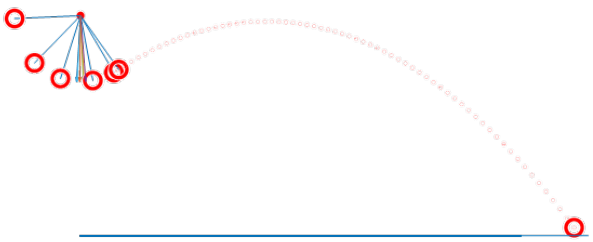

Figure 3.1: Ball Throw task at different times, arrows represent Motor positions

3.1 Ideal Model of the SEA and VSA

The modeling must proceed with the analysis of the basic components and the writing of the energetic terms for the formulation of the Lagrangian. In order to initially simplify the modeling, but above all the identification of the optimal trajectory, we start with the modeling of a SEA device. The VSA model will be obtained by reformulating the equations considering an ideal transmission between spring and end-effector. In the sequel the input is considered as an ideal velocity source and no friction factors exist, to further simplify the system. This further simplification can be made a priori considering that the transfer function between motor torque and its speed follows a higher dynamic than that of the system considered. Clearly this transfer function will depend largely from the control parameters chosen for this application, and this assumption will be verified later in this discussion.

3.1.1 SEA ideal Model

Consider the model depicted in fig(3.2). Starting from this simple scheme we can identify:

$$E_c = \frac{1}{2}J_1\dot{\theta}_1^2 + \frac{1}{2}J_p\dot{\theta}_2^2$$

$$V = \frac{1}{2}K\theta_1^2 + \frac{1}{2}K\theta_2^2 - mglcos\theta_2$$

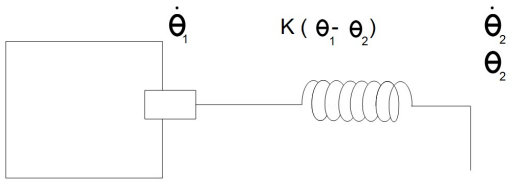

Figure 3.2: SEA diagram

where m is the ball mass, l is the length of the arm and K the stiffness of the spring.

that leads to:

$$\frac{d}{dt}\frac{E_c}{d\dot{\theta}} + \frac{dV}{dt} = u$$

For the sake of simplicity, and in order to reorganize the state variable the same system could also be rewritten as:

$$\theta_1 = \int_0^{t_f} \dot{\theta}_1 dt \qquad\qquad J_p\ddot{\theta}_2 = K(\theta_1 - \theta_2) - mglsin(\theta_2)$$

where J_p is the inertia on the part of the end effector $J_p = J_{arm} + m*(l+r_1)^2$ r_1 being the ball's radius and J_{arm} is the rod's inertia.
Considering the states:

$$x = \begin{bmatrix} \theta_1 \\ \theta_2 \\ \dot{\theta}_2 \end{bmatrix} \qquad \& \qquad u = \dot{\theta}_1$$

3.1.2 VSA ideal Model

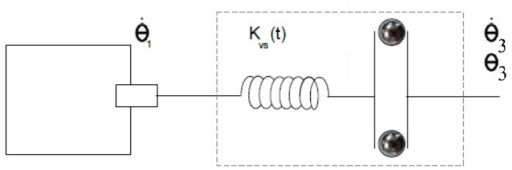

Figure 3.3: VSA diagram

In case of the VSA's ideal model the motor is also considered a velocity source. On the other hand, we will consider the CVT and the spring as one entity as showed in fig (3.3) the stiffness of the combination of CVT and spring resulting in the VSA is $\frac{K}{r}(\theta_1 - \frac{\theta_3}{r})$ where $(\theta_1 - \frac{\theta_3}{r})$is the rotation of the original spring. The variable stiffness$\frac{K}{r}$ will be denoted as $K_{vs}(t)$.

$\theta_1 = \int_0^{t_f} \dot{\theta}_1 dt$ $\qquad\qquad$ $J_{eq}\ddot{\theta}_3 = K_{vs}(t)(\theta_1 - \frac{\theta_3}{r})$

with the control inputs being $u = \left[\dot{\theta}_1 \ ; \ K_{vs}(t)\right]$.

J_eq is the equivalent inertia for the system after the spring $J_{eq} = J_2/r^2 + J_p$
J_2 is the inertia between the spring and the CVT.
In an attempt to show one of the more important characteristic of VSA with the respect to SEA, the graph 3.4 highlights the ideal available stiffness range of each the two, the SEA is constrained by a line which represents the stiffness $\frac{\partial\tau}{\partial\phi}$ where ϕ is the deflection of the spring. The VSA is not constrained by a line rather by an area which is the main advantage of a VSA device. To compare between the SEA and VSA, the torque of each device is defined by the stiffness multiplied by the deflection. The deflection is bounded between 0 and 1.5 rad for both device as it is a characteristic of the spring. On the other hand the stiffness (K for SEA and K/r for VSA) is different for both. Changing r the gear ratio in the VSA outputs different stiffness as we can see in fig(3.4), the max stiffness line is when r is at its minimum and the minimum stiffness line is when r is at it's maximum.

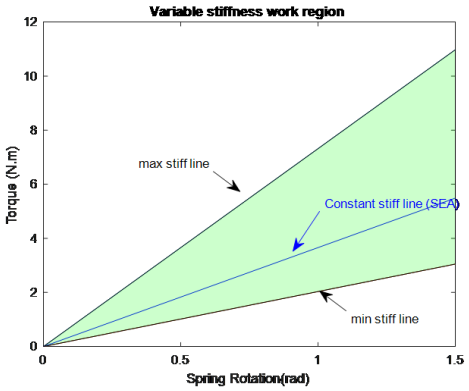

Figure 3.4: Working region of an SEA & VSA

However, choosing which stiffness to apply at each time step is not randomly done and is not a trivial task. In this specific task, it is an optimization problem that requires the optimal stiffness at each time-step to ensure

the system is providing it's highest performance or energy minimization depending on the requirement. In other tasks it could be a specific stiffness that is required by the user which nevertheless gives him a wide range of stiffness choices.

3.2 Trajectory optimization and nonlinear programming

Trajectory optimization is a collection of techniques that are used to find open-loop solutions to an optimal control problem. In other words, the solution to a trajectory optimization problem is a sequence of controls u*(t), given as a function of time, that moves a system from a single initial state to some final state. The resulting solution is open-loop, so it must be combined with a stabilizing controller when applied to a real system [49]. Solving an optimal control problem is not complete without NLP, it is a key element in solving the optimal control problem. One of the algorithms to solve NLP is the interior point method; a class of algorithms that solves constrained optimization problems through solving sequence of approximate problems. They are used to solve convex optimization problems. The basis of this method restricts constraints into the objective function by creating a barrier function, therefore restricting possible solutions to iterate only in the viable region, which results in an efficient algorithm regarding time complexity [50].In order to identify the quantities involved and proceed with the sizing in addition to the model, it is also useful to consider the trajectory that will be performed by the system. Starting from a careful analysis of the state of the art [8][48] it was verified how it is necessary to use an optimization algorithm to identify the ideal trajectory for the launch. This algorithm explained by MathWorks "NLP involves minimizing or maximizing a nonlinear objective function subject to bound constraints, linear constraints, or nonlinear constraints, where the constraints can be inequalities or equalities. Example problems in engineering include analyzing design trade offs, selecting optimal designs, computing optimal trajectories, and portfolio optimization and model calibration in computational finance"[51] . From Mathworks website on nonlinear programming.

For a given state of the system x_0 the goal is to find a control law $u(t, x)$ that minimises the criterion [52] :

$$J(x_0) = h(x(T)) + \int_0^T c(x(t), u(t))\ dt \tag{3.1}$$

T being the final time of the task $t \in [0\ \ T]$

$$\dot{x} = f(t, x(t), u(t)) \qquad \text{System Dynamics}$$
$$c_L \leq c(t, x(t), u(t)) \leq c_L \qquad \text{Path constraints}$$
$$b_L \leq b(t_0, t_f, x(t_0), x(t_F)) \leq b_U \qquad \text{Boundary Conditions}$$

As will be further analyzed hereinafter, the optimization of the trajectory for the thrown problem presented previously leads to the resolution of a non-linear problem that cannot be solved analytically. This leads to the need to find a numerical method for solving. Following a careful analysis, different methods have been found in the literature and many libraries already implemented in Matlab, the tool chosen for our analysis. The choice fell on the optimization library developed by Kelly and presented in [49], where multiple collocation methods can be chosen to optimize the given function. In order to validate the chosen library and in order to choose the correct collocation methods it was decide to start from the analysis presented in [48]. In this work different optimization problems are analyzed both analytically and numerically. The simplest problem analyzed is composed by a simple SEA without gravitational terms:

$$\theta_1 = \int_0^{t_f} \dot{\theta}_1 dt \qquad\qquad J_2\ddot{\theta}_2 = K(\theta_1 - \theta_2)$$

In order to consider on 3.1 the constraints imposed by the dynamics of the system it is convenient to introduce the Hamiltonian:

$$H(x(t), \lambda(t), u(t)) = c(x(t), u(t)) + \lambda^T f(t, x(t), u(t))$$

To maximise the final velocity $h(x(T)) = q(\dot{T})$ and $c(x(t), u(t), t) = 0$ must be set. To solve the optimization problem the following system should be considered:

$$\dot{x} = \frac{\partial H}{\partial \lambda} \tag{3.2}$$

$$\dot{\lambda} = -\frac{\partial H}{\partial x} \tag{3.3}$$

As highlighted in [48] the resolution of this system leads to the typical bang-bang control at the frequency equal to the resonance frequency of the system:

$$\dot{\theta}_{1d} = \dot{\theta}_{1max} sgn(sin(\omega(t - T))) \tag{3.4}$$

where $\dot{\theta}_{1d}$ is the control while $\dot{\theta}_{1max}$ is the maximum possible $\dot{\theta}_1$ value.

Considering this simple case many collocation methods have been tested in order to compare the analytical exact solution with the numerical one.

Finally the Chebyshev orthogonal polynomials, an orthogonal collocation method, has been chosen. Instead of having one segment in the trajectory, this method divides it into multiple segments based on the paper done by [53]. This is computationally fast and has a high precision for high polynomial order and multiple number of segments. It has been decided to start from a big mesh with low precision and kept iterating the solver with a more precise mesh that relies on the results of the previous iteration. For the sake of verifying the correctness of the solver, we compared the analytical solution to the solver's solution, a very high mesh refinement was also applied to check how close can we get to the exact solution.

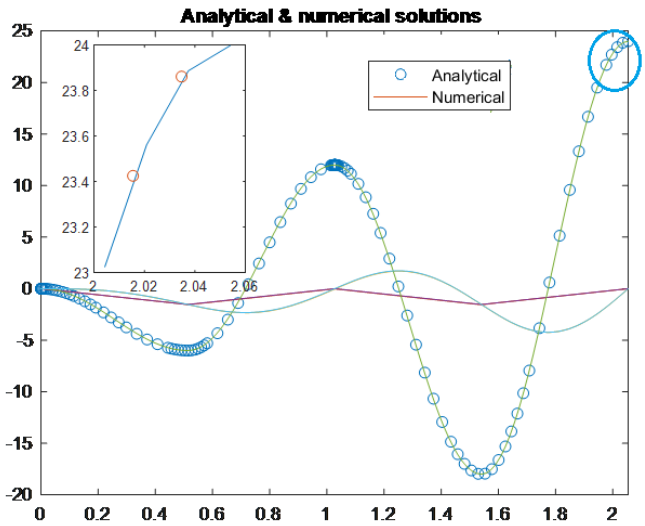

Figure 3.5: Analytical solution vs Numerical solution. the analytical solution is referred to in small circles, we can confirm that the solver is working.

3.2.1 Trajectory optimization

3.2.2 Cost Function

Our optimal trajectory is characterized by exploiting as much energy as possible from the spring throughout the trajectory and to have almost no energy stored prior to throwing the ball (which means the spring released it's previously stored energy). In our ball throwing task, an explosive movement, the goal of the experiment is to maximize the distance thrown by the actuator. Therefore, the algorithm has to find the best angle and highest exit velocity of the ball at the moment of release. This experiment is done

in [30] with a different configuration of VSA, where they also were working on maximizing distance thrown of a ball.

$h(x(T))$ is the terminal cost, and $c(x(t), u(t, x(t)))$ is the running cost. [52] The performance criterion which we previously discussed is formulated into a cost function:

$$J_w = -d(\theta 2(T), \dot{\theta}_2(T)) + \int_0^T -\frac{1}{2} w * ||F(\theta_1, \theta_2)||^2 + \frac{1}{2} R * ||u||^2 \, dt \quad (3.5)$$

The throwing distance d is the terminal cost here and a '-' sign was added in order to achieve the maximum instead of minimum. F being the spring force , u is the motor effort and w & R are their weight numbers that define how much priority each element of the latter is given, respectively. The equation (3.6) is the terminal cost of the distance achieved from the actuator, it can be better visualized in fig.(3.1).

$$d = x_m(\theta_2) + \dot{x}_m(\theta_2, \dot{\theta}_2) T_m(\theta_2, \dot{\theta}_2) \quad (3.6)$$

$$x_m = l \, sin(\theta_2) \quad (3.7)$$

$$y_m = -l \, cos(\theta_2) \quad (3.8)$$

$$T_m = \frac{1}{g} \left(l \, cos(\theta_2) \dot{\theta}_2 + \sqrt{(l \, cos(\theta_2) \dot{\theta}_2)^2 + 2g(y_m - y_0)} \right) \quad (3.9)$$

The problem becomes a ballistic equation where T_m is the flight time of the ball. x_m/y_m denote the horizontal and vertical positions of the ball, respectively.

Constraints

Subject to the dynamics $\dot{x} = f(t, x, u)$ for SEA:

$$f(t, x, u) = \begin{cases} \dot{\theta}_1 \\ \dot{\theta}_2 \\ \frac{K(\theta_1 - \theta_2) - mgl sin\theta_2}{J2} \end{cases}$$

for VSA:

$$f(t, x, u) = \begin{cases} \dot{\theta}_1 \\ \dot{\theta}_3 \\ \frac{\frac{K}{r}(\theta_1 - \frac{\theta_3}{r}) - mgl sin\theta_3}{J_2 * \mu / r^2 + J_3} \end{cases}$$

with

$$-\dot{\theta}_{1_{max}} \leq \dot{\theta}_1 \leq \dot{\theta}_{1_{max}} \qquad \text{Velocity control input limit}$$
$$(\theta_1 - \theta_2) - q < 0 \qquad \text{Maximum spring rotation q}$$
$$x_{min} \leq x \leq x_{max} \qquad \text{States boundaries}$$

$\dot{\theta}_{1_{max}}$ was limited to 3 rad/s
Maximum spring deflection $(\theta_1 - \theta_2)$ is 1.5 rad
θ_2 & θ_1 are bounded by $\pm\frac{\pi}{2}$
A low value for $\dot{\theta}_{1_{max}}$ was chosen since our goal is to highlight the improvement that the addition of a compliant element can give especially for under-powered actuators.
The spring constrained deflection is due to the design of the torsional spring.
The gradient of this inequality path constraint is added in the path constraint with the goal to be as close as possible to a global minimum.

$g(x) = [\theta_1 - \theta_2 - 1.5]$ $\qquad$ $\nabla_{g(x)} = [\frac{\partial g(x)}{\partial t}; \frac{\partial g(x)}{\partial \theta_1}; \frac{\partial g(x)}{\partial \theta_2}; \frac{\partial g(x)}{\partial \dot{\theta}_2}; \frac{\partial g(x)}{\partial u}]$

3.2.3 Parameter identification using optimal trajectory

The system was designed to use torsion springs as energy storage devices. One of the first obstacles is to identify the most suitable spring stiffness for our system. Not to forget other design constraints such as max rotation °, internal diameter, wire diameter, which are limited by spring manufacturing companies' catalogues.
The method used to identify the stiffness, is to iterate the optimal trajectory algorithm with different stiffnesses for each iteration, and check the overall performance of the system. We start by big steps at the first few rounds in order to detect the stiffness range of interest, and this range keeps diminishing until it reaches a suitable resolution of stiffness. The criterion to differentiate between a suitable stiffness and non-suitable is the difference between $\dot{\theta}_2$ and $\dot{\theta}_1$ at time T; it has to be positive and high which is a sign that the spring energy was emptied or used prior to release of the ball (all the potential energy of the spring has been converted to kinetic energy), and another criterion the maximum throwing distance reached which is the terminal goal of our cost function (at the same time taking into account the other parameters mentioned previously for feasibility). The graph 3.6 shows the throwing distance increase proportionally with the stiffness at low values, which show the spring is exploited to the maximum constrained by the motor torque and the maximum allowable spring rotation, until it reaches a maximum point, which is the region containing the optimal stiffness value for the relevant application.

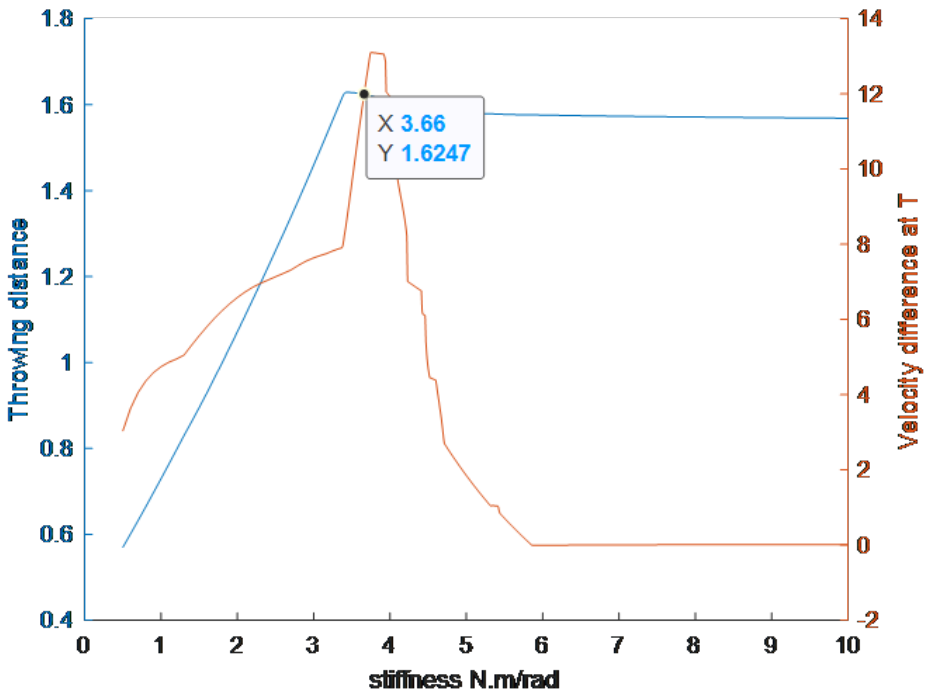

Figure 3.6: Velocity difference & distance thrown vs stiffness

Chapter 4

Mechanical Design & Components

The work shown up to here has dealt with identifying open robotics problem, identifying solutions to overcome these problems and identifying a reference task to experience the advantages of VSA and the proposed technological solution. Some simple models were also presented in order to give to the reader a first contact with the mechanical solution and to identify the main characteristics useful to face the design and sizing of a new setup. Now a new setup will be presented. This setup with a goal to experimentally test the advantages of the VSA-CVT solution. For this purpose in Figure 4.1 the mechanical scheme taken from the CAD model of the new setup is presented. A schematic list of the components used is also presented in the caption. As represented the setup in constituted by a gear-motor system connected by a pulley-belt system to a particular bidirectional elastic element. In turn this is connected to the CVT system, already presented in Chapter 2 and properly modified for this scope.Finally, the output shaft is connected to a sort of end-effector, able to grasp and release a basket ball, the ballistic object. Hereinafter, this work will go into detail of every component in order to better explain the reasons for the choices made and the changes made to the individual components.

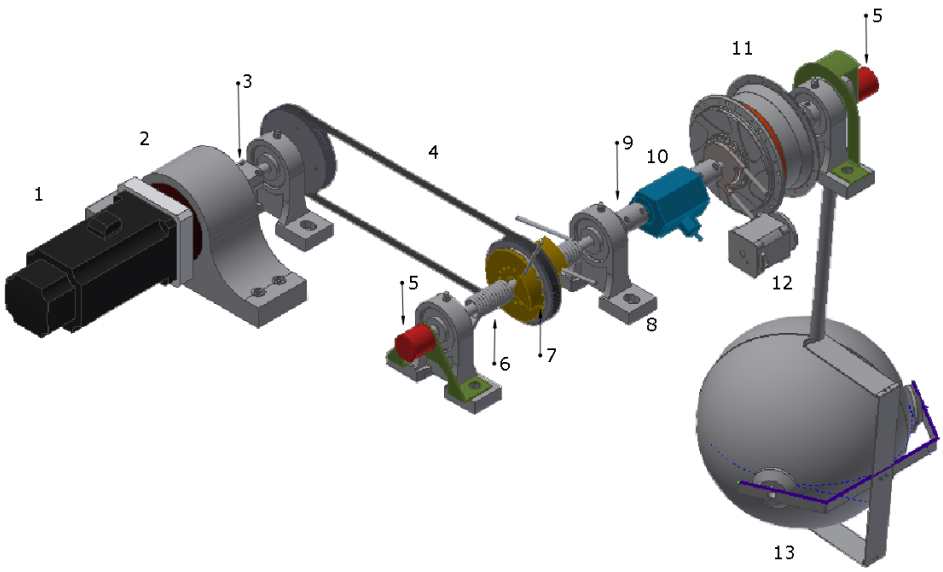

Figure 4.1: 1.Motor 2.Motor Cup holder 3.Motor-shaft coupler 4.Belt-Pulley system 5.Encoder & holder 6.Torsional spring 7.Spring preload mechanism 8.Bearing & housing 9.Shaft Coupler 10.Force sensor 11.CVT 12.Stepper motor & belt-pulley 13.Ball throw mechanism

4.1 Actuators & Sensors

The motor that was used is a Low Voltage brushless servo motor is a SC05DBK from LS mecapion with a planetary gearhead (15:1) and an optical encoder attached to it's back end, which will be used to have position feedback. The table (4.1)shows the motor characteristics.

Table 4.1: Motor Characteristics

Nominal Power (W)	450
Max RPM	5000
Nominal Torque (N.m)	1.43
Max Torque (N.m)	4.25
Velocity constant k_e (V/RPM)	9.8
Torque constant k_t (N.m/A)	0.157
Gear Ratio	15:1
Encoder (ppr)	2500

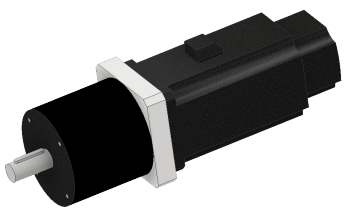

Figure 4.2: Motor, gearhead & encoder

Figure 4.3: CVT gear change mechanism

Figure 4.4: CVT rolling spheres along with their arms

Therefore, with the addition of the gearhead that has an efficiency of 90% at the rated torque[58] the nominal output torque is around 19N.m and the max Velocity is 330RPM.
As will be shown below, in order to complete the task already shown in the previous chapter, it is necessary to carry out a so-called low-level control on the motor. As occurs in almost all automatic applications, this occurs through a feedback control of the kinematic or dynamic parameters. In this particular case, this control is entrusted to a commercial controller (Elmo Gold Cello) capable of carrying out both torque, speed and position controls on the motor. Communication with a central controller will take place via an EtherCat fieldbus. To make sure the position control of the spring ends (θ_1 and θ_2) is resulting in the correct torque estimation, a rotational force sensor (fig4.12) Burster 86-2477 is used for validation.// In addition to the motor's encoder, two encoders (" RE30E-500-213-1") from Copal electronics with 500 ppr are attached on both ends of the CVT. one is attached on the extremity of the shaft before the CVT and the other is attached at the extremity of the output shaft near the end effector shown in (Fig.4.1 element number 5. The reason for choosing two encoders, whereas for the feedback purpose the required amount is just one, is to validate that the CVT is providing the requested gear ratio and to verify and measure eventually the slip through the CVT. The encoder attached to the motor and the end effector encoder are the feedback that is going to be used in the control of the system, and all other sensors are for validation.

4.2 Components

CVT

The CVT presented in this section is the same already shown in the Chapter 2. The CVT changes it's gear ratio by rotating the gear mechanism (fig4.3) that is connected with the rolling spheres (fig.4.4). The gear change occurs when the spheres connecting the input and output of the CVT change their relative rotational axis, which is equivalent to changing the radius of the ball, this shift creates a difference between the rotating radius on the input side and the output side.

Figure 4.5: The components of the CVT from one side

Figure 4.6: The CVT freewheel

Figure 4.7: The CVT coupling

End effector Ball throw mechanism

The ball throwing mechanism having two suction cups to keep the ball attached to the arm during the experiment and abort the suction in the exact time of the launch. The suction cups *7320500000* from Aventics (fig.4.8) were installed in the position opposite to the tangential force shown in (fig.4.10) because referring to the graph in (fig.4.9) the centrifugal (or radial) force is proportional to the square of the velocity on the other hand the tangential force is proportional to the acceleration of the end effector, therefore they were installed in the tangential direction to guarantee holding the non-negligible basketball at all time of the task. The body of the end effector was chosen to be able to withstand the forces from the ball and have a minimal impact on the dynamics of the end effector.

Figure 4.8: Suction cup

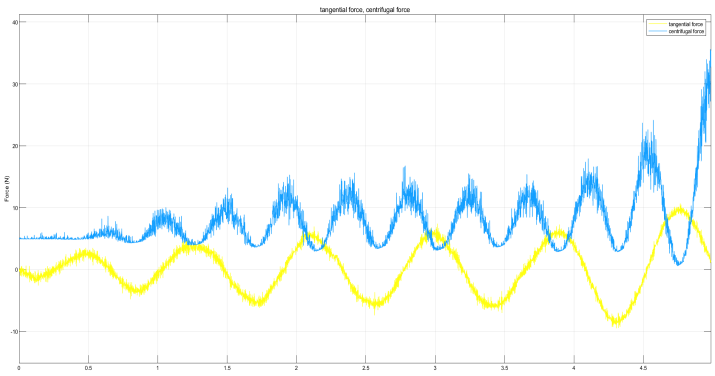

Figure 4.9: Torsional and centrifugal forces on the end effector

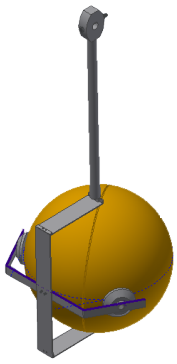

Figure 4.10: End effector

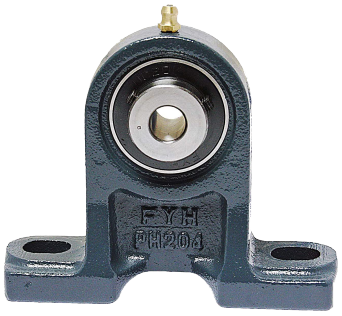

Figure 4.11: Bearing & housing

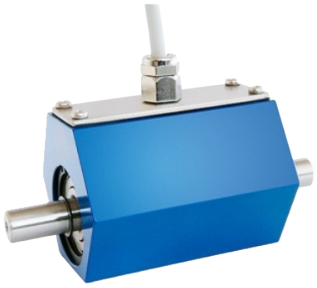

Figure 4.12: Rotational force sensor

Bearings and couplers

The bearings and couplers used to join together the sections of the shaft are commercial. Bearings were chosen according to suitable diameter, working rpm and forces applied to it (fig4.11). The couplers ("721.25.3232") from Huco were chosen according to their diameter and nominal torque.

Torsional Springs

The elastic element is composed by a quite complex mechanical system. Tt is mainly composed by two helical torsion springs. The spring stiffness optimization was done in the previous chapter resulted in specific characteristics of the springs. Unfortunately, in the real world parameters are most of the time not available as precisely needed, so the closest model to what was obtained in the results should be chosen. The torsional spring that was chosen is "G.255.400.0950" from Vanel and has very close parameters to the ideal one.

Belt and Pulley

The Belt and pulley used between motor and the system are:
500 mm belt (10 / T5 / 500 SS) from Contitech and two 36 teeth pulleys with 5 mm pitch (286-5708) from RS-PRO. A belt tensioner was taken into consideration but it was not included in the CAD model.
The synchronous belt and pulley system was used because it was the most convenient system for the design that could transmit high torque. The load of the belt and pulley was calculated based on the max torque in the system, the pulley diameter and the belt's max load.

Stepper motor

A Nema 16 stepper motor with a belt and pulley is used to change the gear ratio of the CVT, an alternative to the classical bicycle rotational gear change by hand.

Stepper motor turned out to be the most useful choice for this particular application. The absence of feedback sensors makes this type of motor easy and cheap

to manage. The only problem to be addressed in practice is the need to refer the current position of the motor with the real transmission ratio. In this sense, the redundant use of the position sensors upstream and downstream of the CVT, help in this scope.

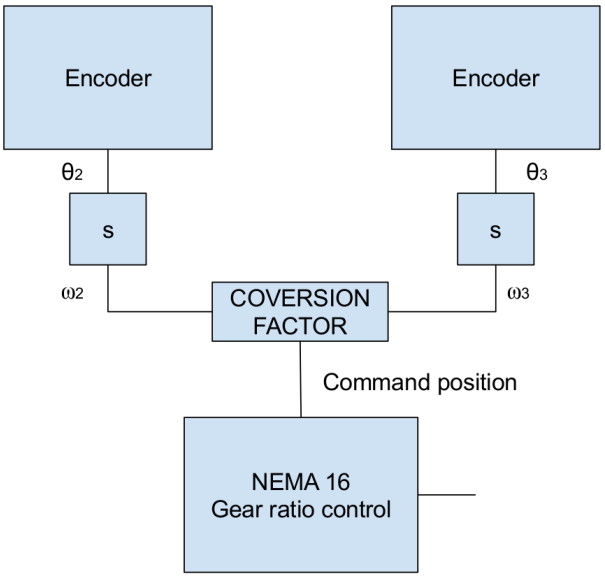

Figure 4.13: Gear feedback system. θ_2 represents the position before the CVT, while ω_2 being it's derivative. The subscribe 3 represent position and velocity after the CVT. The conversion factor represents the transform from gear ratio to motor position

4.3 Mechanical Design procedure

4.3.1 Shaft design and sizing

The maximum torque the motor can transmit is 19Nm, but in the task the maximum torque reached is around 6Nm. However to be conservative, a safety factor of 2 was used when considering the torque, in case something goes wrong while experimenting so the system doesn't fail. Two materials were considered for the shaft, Aluminum and low carbon Steel with a maximum shear stress of 50 Mpa and 200 Mpa respectively.

Since the major stress on the shaft is due to the torque by the motor, it was the only factor considered, however the diameter will be increased a bit to account for other factors.

$$\tau = \frac{T * c}{\pi/2 * c^4} \tag{4.1}$$

Where T is the torque, τ is the stress and c is the radius of the shaft.
The minimum shaft diameter, accounting for torsional shear stress only, for Aluminum is 11.5 mm and 7 mm for Steel. However, larger diameters are considered

for safety and availability of components with similar dimensions. The shaft dimensions finally chosen are 10mm & 12mm low carbon steel varying throughout, because of the constraint of some commercial components.

4.4 Encountered Problems & Solutions

4.4.1 Bidirectional spring and preload system

Two torsional springs system

The compliant element used in this task are two single torsional springs, but since the task requires torque transmission bidirectionally and a torsional spring can only transmit torque in one direction(to prevent plastic deformation of the spring), two torsional springs had to be used where both of them work accordingly and are preloaded at the zeros position in order to avoid singularity in the springs and avoid backlash. The motor has to be attached to both spring ends and both of them have to be attached to the output, on the other hand when the motor is rotating in one direction only one spring has to rotate along with it (fig.4.14). Different solutions have been discussed, but some of them were very complex in terms of manufacturing so we opted out for a more simple solution that nevertheless does the job. The main constraint is that the springs have to both be attached to the motor shaft and the input shaft of the CVT from each end, respectively. To do so, the motor transmits torque through a belt and pulley system (Fig.4.15), the second pulley is connected to both springs from each side.
On the other ends of the springs, they are both connected to the output shaft which passes inside the pulley through a bearing and inside the springs. Each spring transfers the torque to the shaft through a pin Fig.(4.16) that transmits it to the shaft (opposite directions for each spring), the pin is fixed with a screw to keep it from moving. The shaft sits inside two bearing holders at each end. The

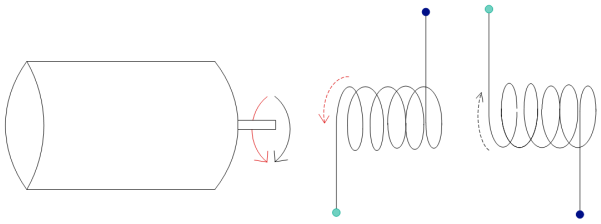

Figure 4.14: Motor-Springs direction of rotation

pulley was chosen because it simplified the problem in terms of shaft design, because other solutions for example required two different shafts with different dimensions that were rotating independently of each other, one shaft between motor and spring and the other between spring and output. The tricky part was that the springs had both to be connected to the same output shaft and the same input shaft. To make a

comparison, in this design the pulley is replacing the first shaft and easing the way to the motor to be connected to both springs. This can be visualized in (fig.4.14) where each direction of rotation of the motor is related to one of the springs as shown, on the other hand the colored circles show where each end of the spring belongs to, for example the light blue circle is for the ends of the springs that are connected to the motor shaft and the dark blue circles are connected to the input of the CVT.

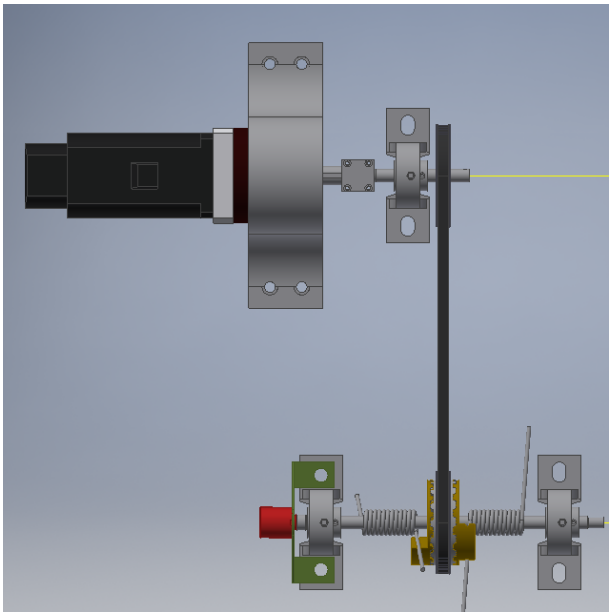

Figure 4.15: Top view of motor-bi-directional torsional spring shaft

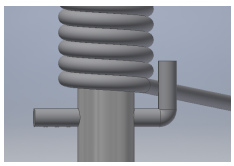

Figure 4.16: Spring-Pin-shaft

Pre-load mechanism for the springs

This mechanism is attached to the pulley from both sides, one for each spring. Each part is constituted of 2 parts, one is responsible for attaching to the pulley through four threaded holes. The second part transmits the torque to the spring and is meshed to the first part through teeth that mesh inside each other and they are also screwed together. The reason for the multiple holes that can be seen in

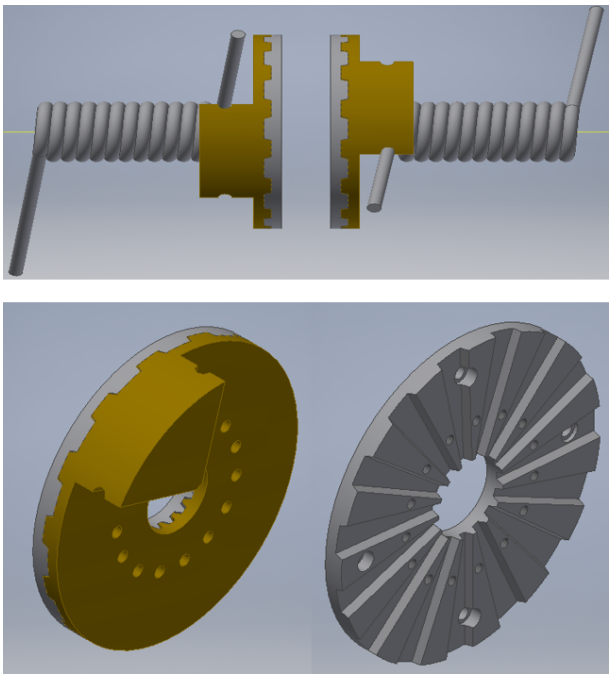

Figure 4.17: Springs preload mechanism

(fig.4.17) is to have small angle difference to be able to choose from to preload the springs. An exploded view shows the whole mechanism to better understand (fig.4.18).

Unidirectional CVT

The CVT under study is a Nuvinci N380 used for bikes explained in detail in Chapter 2, transmits torque in a single direction. Starting from the analysis done on the mechanisms included in the transmission, it was concluded that a freewheel mechanism was installed on one side of the CVT. The side of the CVT related to the freewheel was disassembled (fig.4.5) and taking it apart and removing the freewheel (fig.4.6), which was thought to be the only factor making the CVT transmit torque in one direction. However, another problem was encountered. It was found that the CVT had a coupling (fig.4.7) that connects the input to the transmission, it had teeth shaped in a way to fully transmit torque in only one direction and slip in the other direction, so it had to be changed to a coupling that transmits torque both ways.

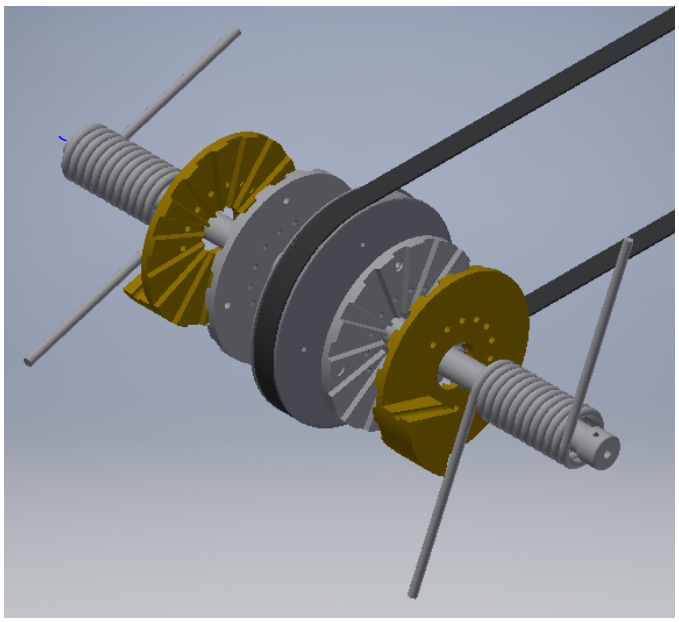

Figure 4.18: Preload mechanism exploded view

Chapter 5

Estimated real model & Control

Several models could be considered for a same system. In chapter 2, was shown a very simple model, which allowed to reach some preliminary results useful for the design and sizing of the main components, given the task described. In this chapter the modeling will be revised, considering all those characteristics of the various components not considered previously. The chapter was supposed to end with a comparison between these models presented and the experimental results. Unfortunately, the explosion of the global pandemic did not allow the tests to be carried out and the results to be compared.

5.1 Motor

By observing the system as described in Chapter 4, one of the main elements is represented by the electrical motor. The analysis carried out in Chapter 2 did not deal with motor modeling, considering it as an ideal speed generator, not subject to friction or other physical phenomena. To proceed with a complete description of an electric motor both the electrical and mechanical parts and the interactions between them must be considered. From the electrical point of view, the motor is a brushless with the three phases on the stator that allows to create a rotating field which in turn induces the rotation of the stator. The complete electromechanical description should therefore take into consideration the three phases and their interaction in the rotation magnetic field generation. Such a complete description goes beyond the purposes of this thesis, for this reason it's chosen a simpler modeling like the one used for brushed DC motors

$$L\frac{di}{dt} + Ri + k_e n\dot{\theta}_1 = V \tag{5.1}$$

where L represent the winding inductance, R is the winding resistance, k_e is the electric constant that that return the electromotive force, stated the rotation speed of the motor. All these parameters will be verified in the next experimental phase.

At the moment the parameters described in Chapter 4 for a single phase will be used.

The motor is also constituted by a gearhead with a *15:1* reduction ratio (indicated with n in the previous formula and in the sequel). The gearhead will also be characterized by its own inertia (J_g) and its own friction (D_r).

$$(J_m * n^2 + Jg)\ddot{\theta_1} + D_r\dot{\theta_1} = T_m * n \tag{5.2}$$

where T_m is the torque generated by the motor while J_m is the motor inertia. In order to simplify this equation, we can use:

$$J_1 = J_m * n^2 + Jg$$

J_m is the motor inertia and J_g is the gear reduction inertia and V is the input voltage and i is the current.

$$u = T_m * n \tag{5.3}$$

$$u = k_t \frac{V - k_e n\dot{\theta_1}}{R} \tag{5.4}$$

To start with control design and analysis it was considered to start with a simpler model w.r.t the final CVT-VSA system. For this reason the analysis start with the SEA model and checking it's behaviour with different control strategies, it will be possible to get important information regarding the final VSA model.

5.1.1 SEA model

As already stated, the SEA setup is constituted by just a single elastic element with a constant stiffness. After some consideration, not reported here for sake of brevity, it was decided to consider an inductance value $L = 0$. The choice could also be justified considering that the electrical eigenvalues are in general faster than the mechanical one. This premise took to rewrite the motor equation as:

$$Ri + k_e n\dot{\theta_1} = V \tag{5.5}$$

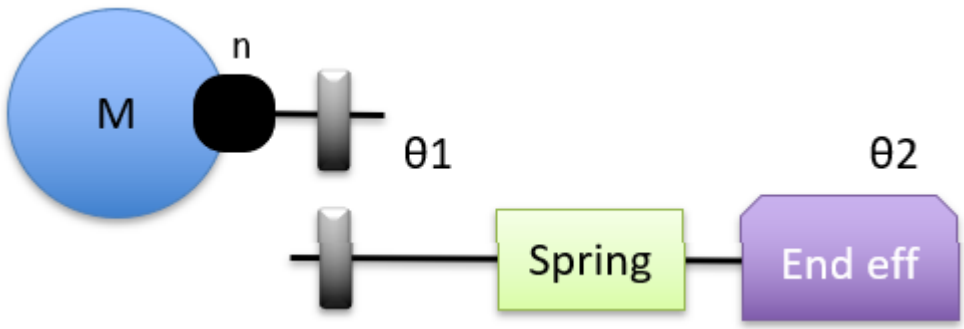

Figure 5.1: Serial Elastic Actuator model

$$\ddot{\theta}_1 = \frac{K(\theta_2 - \theta_1) + T_m n}{J_1} \tag{5.6}$$

with $T_m = k_t i$ the motor torque.

$$\ddot{\theta}_2 = \frac{K(\theta_1 - \theta_2) - mglsin\theta_2}{J_2} \tag{5.7}$$

Combining (5.1) with (5.4) to get the motor voltage as an input, in order for the motor dynamics to be taken into consideration.

$$\ddot{\theta}_1 = \frac{K(\theta_2 - \theta_1) + k_t \frac{(V - k_e n \dot{\theta}_1)}{R})}{J_1} \tag{5.8}$$

where m is the ball mass, l is the length of the arm and K the stiffness of the spring and n is the reduction ratio.

5.1.2 VSA Model

VSA model should represent the model closest to the final setup. The motor dynamics will be taken into consideration as already done for SEA model. The efficiency of the CVT is taken into consideration. In our model the efficiency will affect the output torque value and in turn the output power. The spring and CVT were considered as one entity for the sake of simplicity. To model the CVT an inertia will also be taken in consideration. θ_2 is the angular rotation on the spring output,

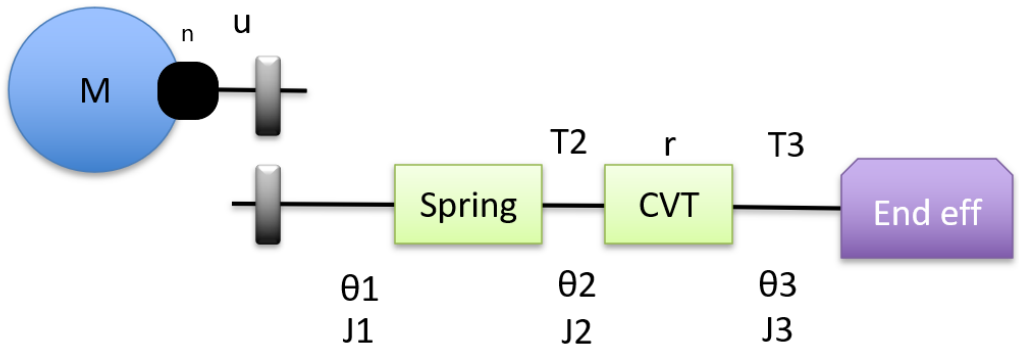

Figure 5.2: Variable stiffness actuator model

θ_3 is the angular rotation of the CVT output. θ_2 and θ_3 are linearly proportional with respect to the gear ratio r fixed by the system described in Chapter 4. From this considerations it is possible to write $\theta_3 = r\theta_2$ as the CVT kinematic equation.

$$\ddot{\theta}_1 = \frac{u - K(\theta_1 - \theta_2)}{J_1} \tag{5.9}$$

$$\ddot{\theta}_2 = \frac{K(\theta_1 - \theta_2) - T_2}{J_2} \tag{5.10}$$

$$\ddot{\theta}_3 = \frac{T_3 - mglsin(\theta_3)}{J_3} \tag{5.11}$$

$$\theta_3 = r * \theta_2 \tag{5.12}$$

The efficiency will affect the output torque and power in this sense.

$$T_3 = -\frac{T_2 * \mu}{r} \tag{5.13}$$

Could be useful to note that this equation could be applied just in case of "positive" power, considering that the power flow from the motor side to the end effector side. In case of "negative" power, the equation must be modified to:

$$T_2 = -T_3 r \mu \tag{5.14}$$

substituting (5.4), (5.10), (5.12), (5.13) and (5.14) in (5.9) and (5.11)

$$\ddot{\theta}_1 = \frac{(k_t \frac{V - k_e n \dot{\theta}_1}{R}) - K(\theta_1 - \frac{\theta_3}{r})}{J_1} \tag{5.15}$$

$$\ddot{\theta}_3(J_3 + \frac{J_2 * \mu}{r^2}) - \frac{K * \mu}{r}(\theta_1 - \frac{\theta_3}{r}) + mglsin\theta_3 = 0 \tag{5.16}$$

$$\ddot{\theta}_3 = \frac{\frac{K*\mu}{r}(\theta_1 - \frac{\theta_3}{r}) - mglsin\theta_3}{J_3 + \frac{J_2*\mu}{r^2}} \tag{5.17}$$

T_2 being the coupling torque between the spring and the CVT, T_3 is the torque between the CVT and the end effector. The manufacturing company did not disclose the efficiency μ of the transmitted torque of the CVT, it is considered to be 90% on average according to the tests conducted by [54] on rolling traction CVTs for 8 Ball cavity devices and gear ratios between 0.5 & 1.8 .

5.2 Control

The control strategy adopted includes a high level control and low level control, where the high level controller is concerned with trajectory tracking, having the states as feedback it can control the error of each state w.r.t the trajectory. It outputs a desired torque which is interpreted by a low level torque control that formulates the problem into a position control problem thanks to the compliant element in between.

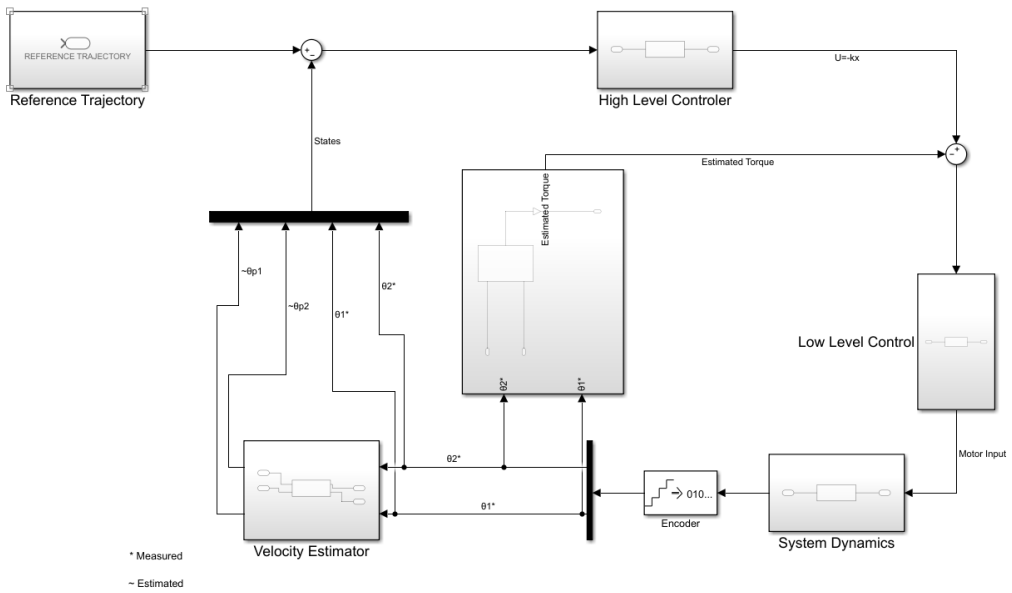

Figure 5.3: Control strategy

As we can see from the block diagram (fig.5.3), the optimized reference trajectory previously calculated is fed to the high level controller, an optimal controller, and a desired torque is fed to the low level controller. The output from the low level controller is the input torque to the motor, which the latter can be transformed to an input voltage referring to (eq.(5.4)).

5.2.1 Low Level Control

The low level control strategy is based on the study by Heike Vallery[55] that applies a torque control on a SEA, inspired by the method used by Pratt [56] and [57]. The control strategy can be summarized by the control scheme depicted in (fig. 5.4).

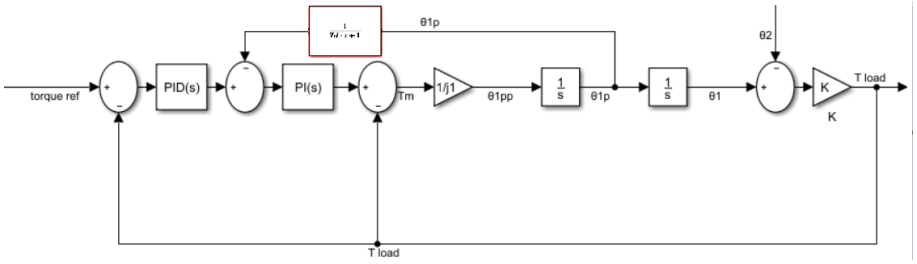

Figure 5.4: Serial Elastic Actuator low level torque control illustration

The high level control produces a desired torque that satisfies the tracking. This desired torque is an input to the low level controller. The actual load torque on the motor, which is calculated from the spring deflection, is subtracted from the desired torque and fed into a PID controller which outputs a desired motor velocity. $\dot{\theta}_{1_{des}} = PID(T_{Load_{des}} - T_{Load})$

The actual velocity is then subtracted from the desired velocity and fed to a PI controller that represent the internal motor controller. As already said in Chapter 4 this velocity or position control loop is already implemented in the motor driver chosen.

The term $T_d s + 1$ is added because an encoder is used to estimate the velocity which causes a measurement delay. This controller relies on position control to control the torque which gives it an advantage since it doesn't require a force sensor. This represent a big plus compared with the "classical" force controller used in automation. As stated in Chapter 2, the force sensor measures are in general derived from a strain gauge sensor. This kind of sensors has in general a moderate noise that decreases with increasing amplifier quality (and cost) . This noise must be filtered in some way and this involves a delay in the force sensor measure. Using the position value to estimate the force, is it possible to refer to a digital signal that doesn't compromise this problem related to the amplifier noise. This is a big advantage in terms of measure readiness and response speed of the system.

The force estimation could be also used for safety reasons. The task considered doesn't expect the human presence or in general doesn't consider the possibility of an obstacle to suddenly obstruct the end-effector movements. In this case the torque measure and the readiness of the control loop is crucial to obtain a safety behaviour both for human and robot. This particular case will be not considered in the rest of this text. In any case, this low-level controller has been thought of also in these terms.

The parameters of the two controllers (PI and PID) have been bounded by simple rules in [55] to obtain both a good tracking and a good noise rejection by the controller.

5.2.2 High Level Control

In the high level control, a time-varying finite horizon Linear Quadratic Regulator (LQR) is used that accounts for the non linearities of the system (which are caused by the non-negligible angles of motion of the end effector and the gear ratio of the CVT) by calculating the piece-wise linear dynamics of the system and forming a linearized state matrix A at each. The differential Riccati equation is calculated and variable gains are obtained throughout the task. The reference trajectory previously calculated was introduced here in the variable

$$x_{ref} = [\dot{\theta}_{1_{ref}}\ \theta_{1_{ref}}\ \dot{\theta}_{2_{ref}}\ \theta_{2_{ref}}]^T$$

(5.18)

The LQR (5.19) is solved along the trajectory, where the A matrix is continuously changing due to the nonlinearities of the system, therefore it is calculated at each time step to be included in the differential Riccati equation to obtain the time-variant gains.

$$J = (x(T)-x_{ref}(T))^T \frac{w}{2}(x(T)-x_{ref}(T))+\int_0^T (x(t)-x_{ref}(t))^T Q(x(t)-x_{ref}(t))+u_c(t)Ru_c(t)\ dt \tag{5.19}$$

where R is control weighing matrix, w is the terminal state target matrix and Q is the state weighing matrix.

The output from the controller is the torque input to the low level controller u=-Kx. The gear ratio of the CVT is considered as a feedforward input, it is fed to the system based on the optimization task.

The gain vector K shown in (fig 5.5) and (fig5.6) is variable throughout the trajectories in (fig.6.5) and (fig6.7). As can be seen from the graphs there are two orders of magnitude for the gains (very high gains on kx2 which is for θ_1) because the weight matrix Q was chosen to have very high weight on only θ_1 and 0 for other values, because the system can be controlled through controlling θ_1 by knowing the system dynamics. The gains drop at the end of the simulation, this is due to the w weight matrix, it was chosen with a very small gain (relative to the values chosen in Q and R) on the state θ_2 therefore it did not have much effect on the control, however if the terminal value is required to be very precise on a state the weight can be highly increased and the controller gains for that specific state will highly increase towards the end of the task.

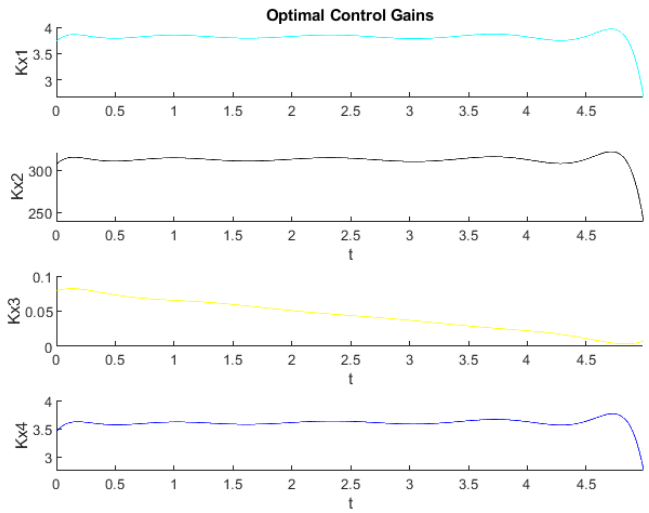

Figure 5.5: Gains varying throughout the simulation for SEA, respectively for $\dot{\theta}_1\ \theta_1\ \dot{\theta}_2\ \theta_2$

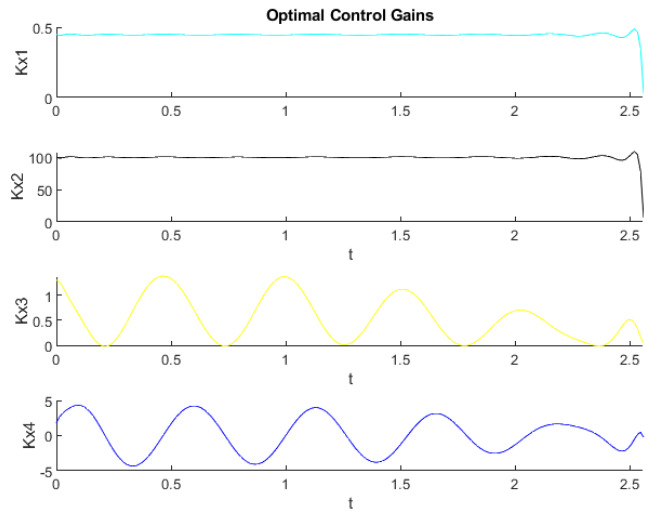

Figure 5.6: Gains varying throughout the simulation for VSA respectively for $\dot{\theta}_1\ \theta_1\ \dot{\theta}_2\ \theta_2$

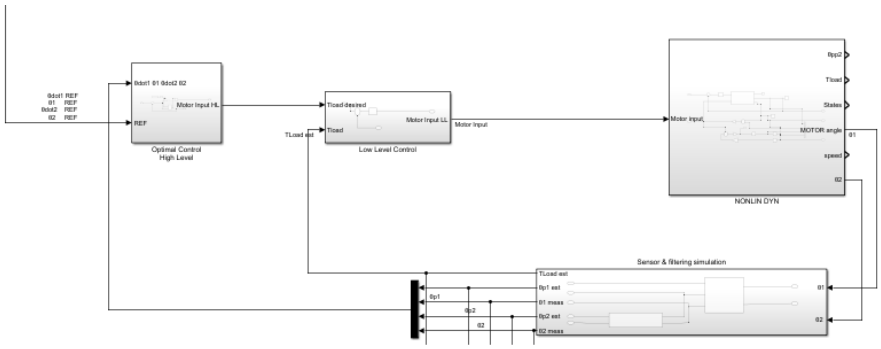

Figure 5.7: Low level & High level Control Block diagram on Simulink

The (fig.5.7) shows the control block diagram on Simulink, it can be seen that only two sensors are providing feedback, however there are 5 signal feedbacks to the low level control (Torque) and high level control (the four states), this is because the velocities and torque load are estimated from the rotational angles measured by the encoders.

5.3 Simulation

Measured signals and Velocity estimator

Noise signals have been added to rotational angles (since they are the measured signals) to simulate the real process. Noises are always present in a real system, so it is applied in the simulation to verify the noise rejection.

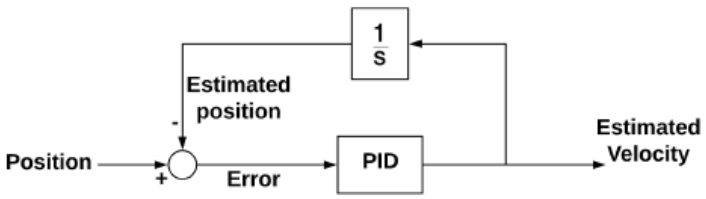

Figure 5.8: Velocity estimator

The rotational velocities have been estimated by applying a feedback loop with a PI controller to the measured position by the encoder (fig.5.8). This estimator acts as a linear low pass filter. The advantages of this estimator is that it is easier to implement in real applications, parameter tuning is more adaptable to the user and it has a good compromise between simplicity and performance.

5.3.1 Results SEA

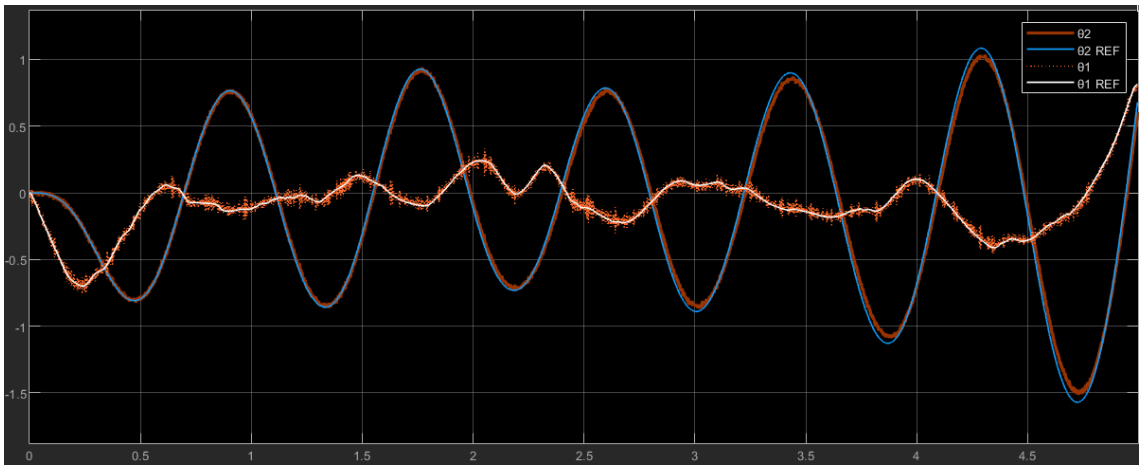

Figure 5.9: Rotation angles Simulation result

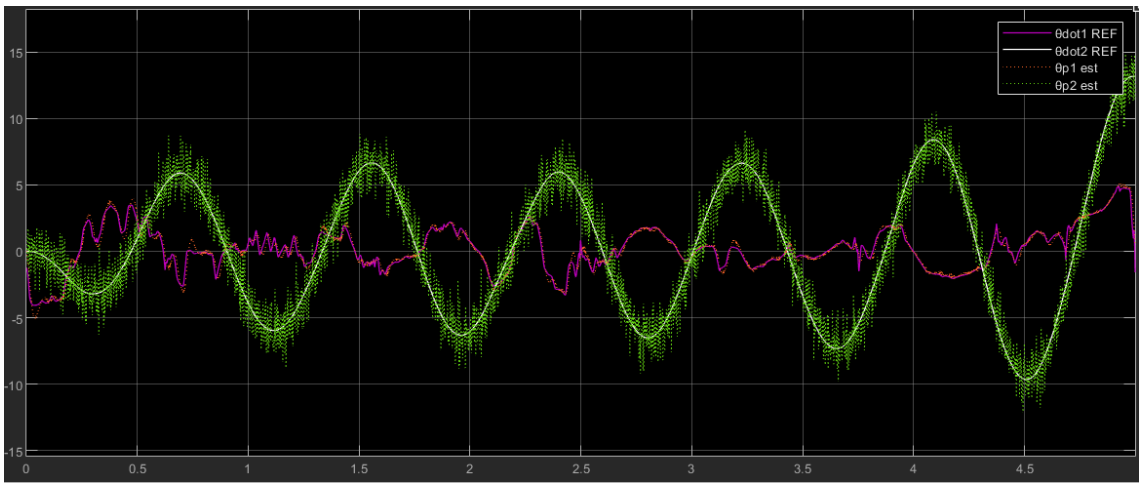

Figure 5.10: Rotational Velocities Simulation result

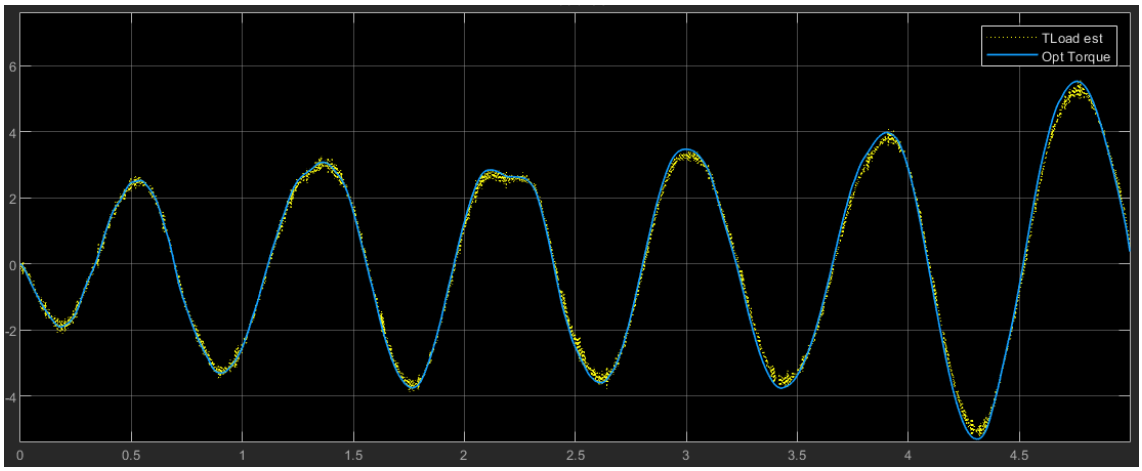

Figure 5.11: Estimated Torque & Optimal Torque

θ_1 is tracked with a trivial delay stated that Q matrix has high weights on θ_1. $\dot{\theta}_1$ is also tracked with an insignificant delay derived from the great performance on θ_1 tracking. The advantage in tracking position in this case is due to the direct position measure from the sensor. Using speed as the feedback signal would have led to an intrinsic delay due to the velocity estimation. On the other hand, the low level controller is controlling the torque, based on the position difference $(\theta_1 - \theta_2)$, so to get a good tracking of θ_2 it is required to get a very good torque control.

5.3.2 Results VSA

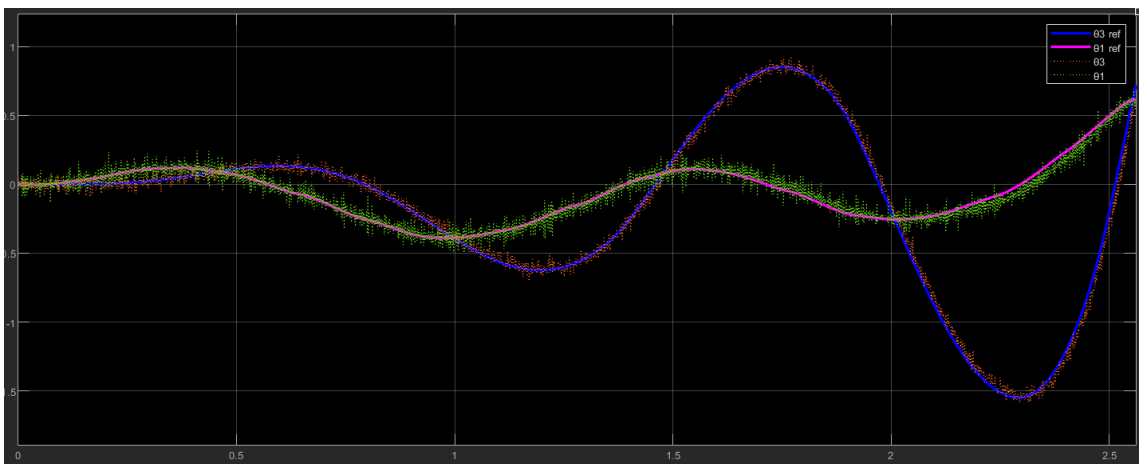

Figure 5.12: Rotation Simulation result

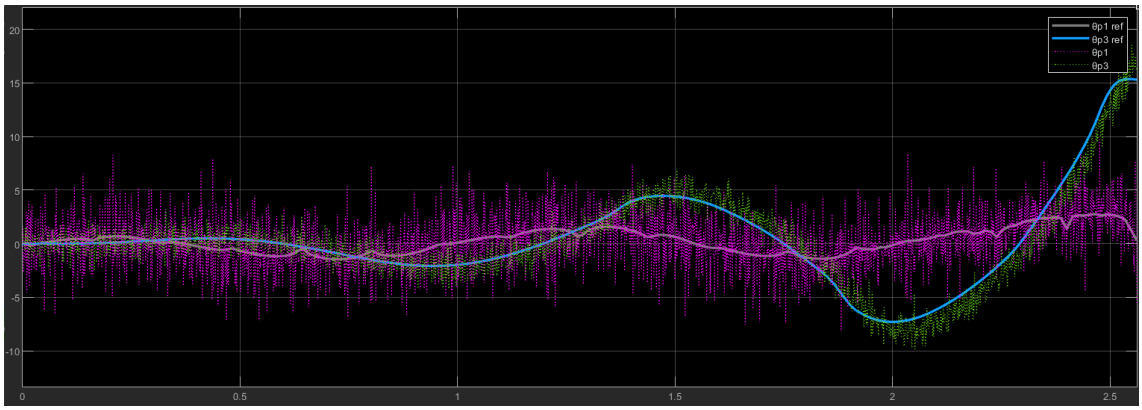

Figure 5.13: Velocity Simulation result

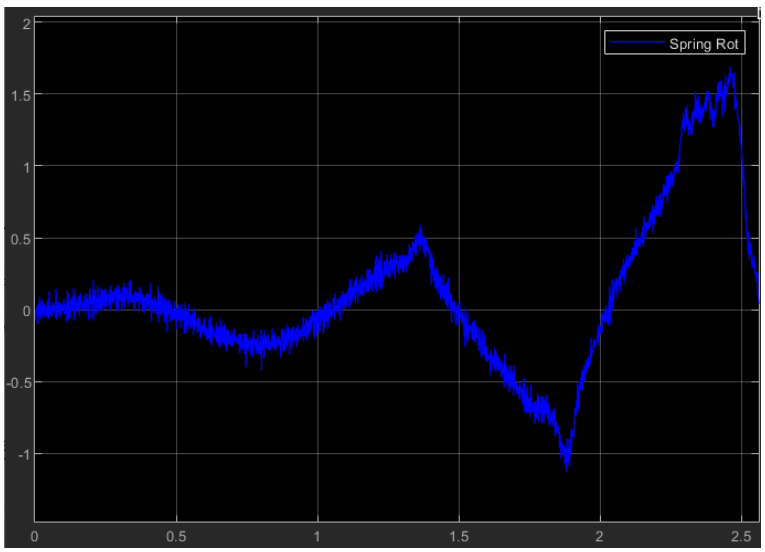

Figure 5.14: Spring deflection during simulation

It can be seen from the graph (fig.5.12) that there's a delay of 5ms in the rotational tracking due to the controller and a slightly higher delay of 12ms in the velocity tracking (fig5.13) due to the controller and the extra delay is due to the velocity estimator.

5.4 Final discussion

The trajectory is well tracked by the controller in both models. The model refinement was not possible since we had no physical parameters from the real components which is a critical step to get a model as close as possible to the real one.

Referring to the graphs of the spring rotation in (fig.5.14) for VSA and SEA it can be seen that the deflection in the simulation is not surpassing the maxi-

mum allowed spring rotation and the constraints are respected, which shows that the torque in the system is uniform with the optimal torque from the reference trajectory.

Chapter 6

Comparison between VSA, SEA & a traditional rigid actuator.

This chapter compares the three classes of actuators: rigid actuator, SEA and VSA. The comparison will be based on performance and energy consumption of the different devices. The comparison shall take into account the characteristics of these three kinds of actuators. In order to find the optimal trajectory in Chapter 3, a speed limited ideal motor was considered, so no torque limit was used. Now, to make a fair comparison between these different kinds of actuators, the motor-gearhead group, included in every system, will be considered. As can be seen in Chapter 4, the nominal power of the motor is absolutely much greater than the one required from the experiment. For this reason the motor power will be limited to 15W. The time for the experiment has not been strictly limited to a fixed value to not over-constrain to a specific time (since the SEA and VSA are working on different stiffness therefore the oscillation period for each device varies) but it was limited between 2 and 5 seconds, and the suitable time is calculated by the solver depending on the optimization.

6.1 Performance comparison

The comparison will be based on the same goal: the maximum throwing distance achieved. This gives us an idea about how the system is exploiting the potential of the elastic system by making an explosive movement. The first device that will be analysed will be called rigid actuator (motor+gearhead) and will be composed simply by the electrical motor rigidly attached to the end-effector. SEA and VSA systems were extensively presented during Chapter 3 and 5. The maximum position for θ_1 will be limited between $\pi/2$ and $-\pi/2$. This is made for practical reason due to the difficulties that arise from using a bigger range.

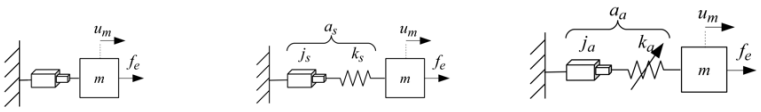

Figure 6.1: The different devices under test

6.1.1 Rigid Actuator

In the rigid actuator, it can be seen that on the 2.5s the actuator takes the end effector to the max negative angle $(-\pi/2)$ extending its range of movement and also by doing this it's increasing its potential energy by lifting the ball to a highest position (fig.6.4). Then it accelerates at 3s to maximize the velocity before release (fig.6.2). It exploits the maximum position it can in order to be able to have enough time to reach it's maximum velocity, the final velocity reached is $9.7745 rad/s$.

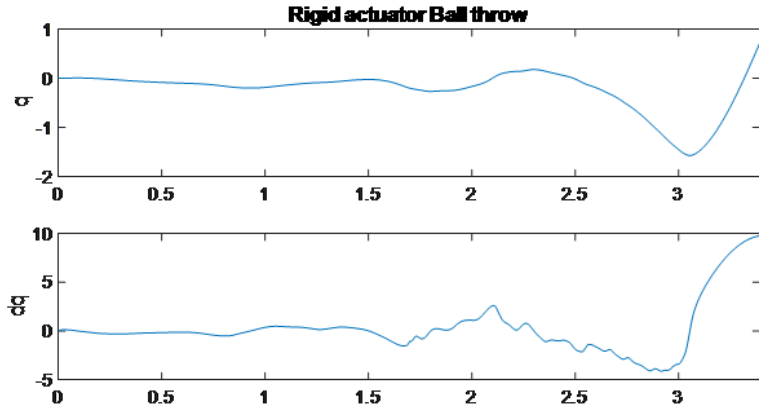

Figure 6.2: Simulated optimal trajectory for rigid actuator (Rotation, Velocity)

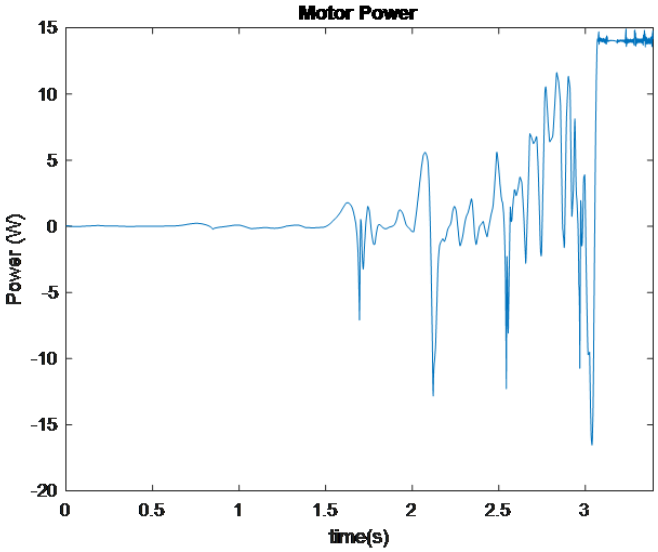

Figure 6.3: Instantaneous motor power

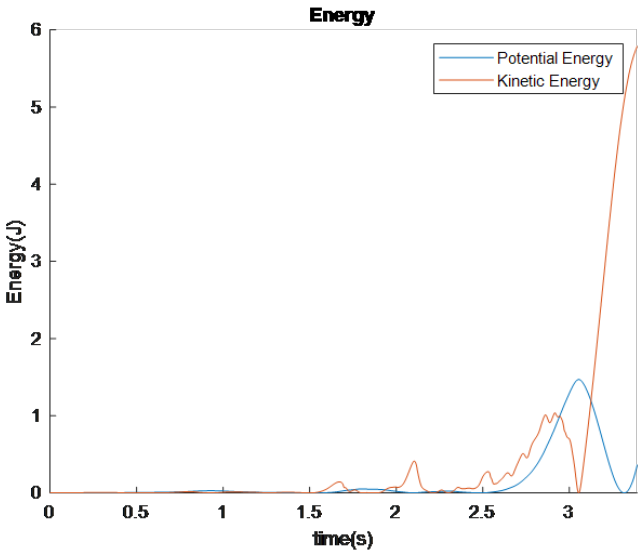

Figure 6.4: Kinetic and potential energies for rigid actuator

6.1.2 Series Elastic Actuator

In this case the actuator is composed of the same motor used in the rigid actuator but a spring was added which allows it to store elastic energy and release it during the launch phase.

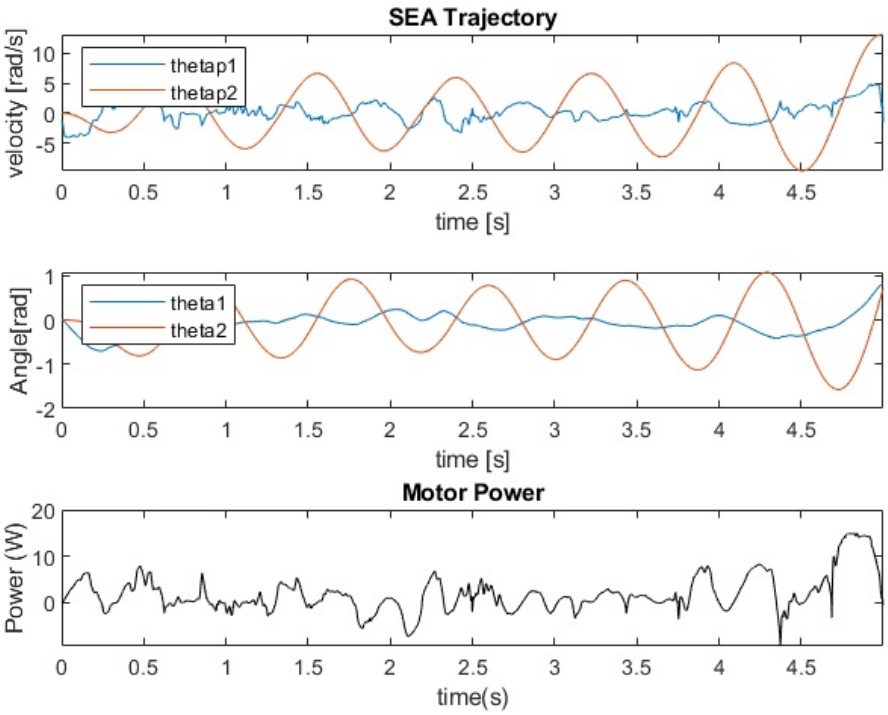

Figure 6.5: Simulated optimal trajectory for SEA device

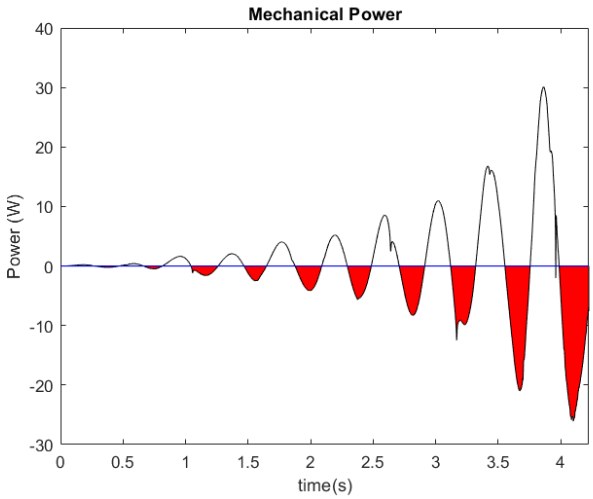

Figure 6.6: Simulated Mechanical Power on the output

Referring to (fig.6.6), the area in red is the stored energy by the spring (numerical integration of the power). It can be seen that this energy increases throughout the trajectory until the last oscillation where it is maximized to be used completely prior to release. Although the maximum power by the motor is limited to 15W in this task, due to the presence of a spring, the SEA was able to provide more power in the last oscillation to maximize the throwing distance and the final velocity (fig.6.5). The maximum final velocity at the end-effector reached is $13.1289 rad/s$. So it is possible to state that the system is able to store energy in a first phase and release it in the following phase. This released power will be summed to the motor power in the launching phase.

6.1.3 Variable Stiffness Actuator

As described in Chapter 4 VSA has a spring and in addition has the ability to continuously vary the CVT ratio and consequently the stiffness of the spring (fig.6.8)).

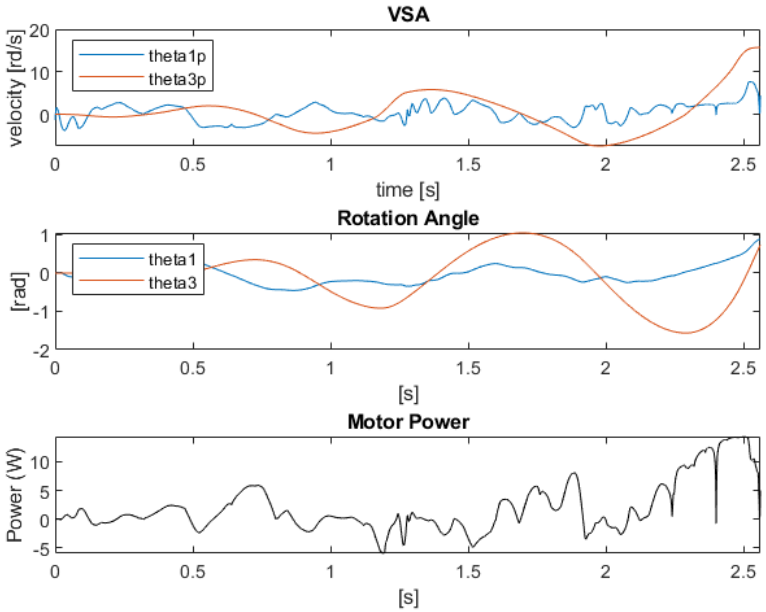

Figure 6.7: Simulated optimal trajectory for VSA device

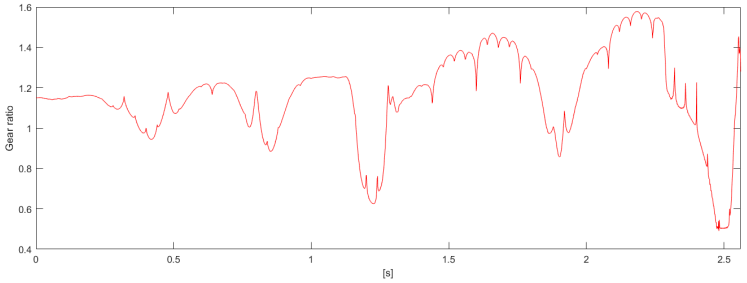

Figure 6.8: Simulated optimal gear ratio for the VSA

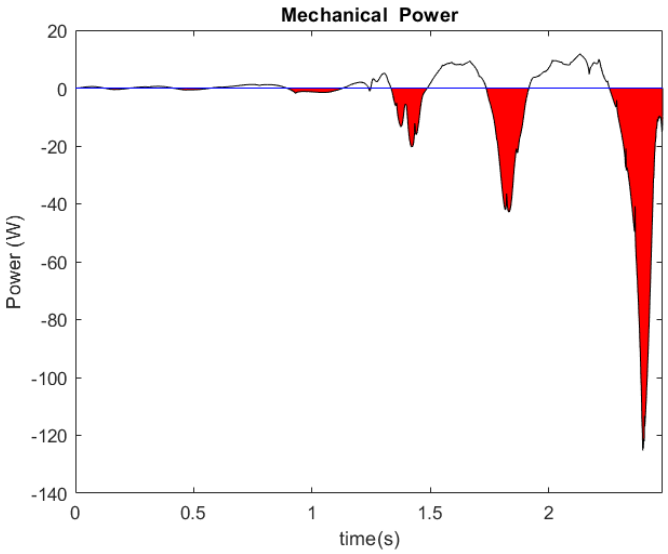

Figure 6.9: Simulated mechanical power for VSA limited power

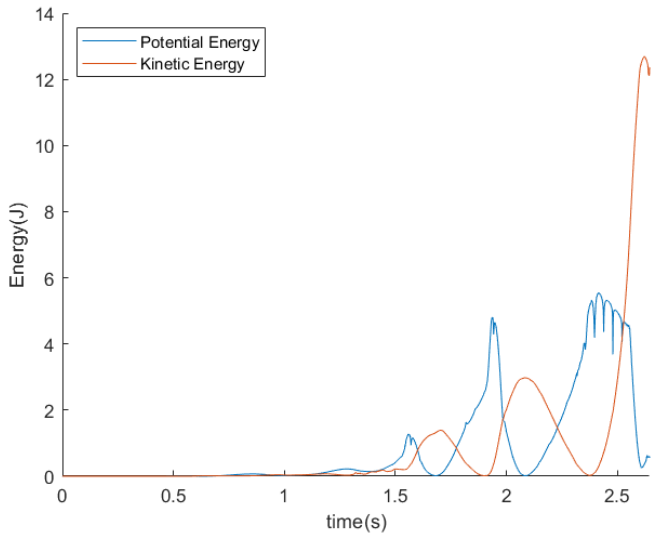

Figure 6.10: Simulated Kinetic and Potential energies for VSA device

The elastic element stores a significant amount of energy throughout the task since it has the ability to always get the optimal stiffness. This makes it more efficient to store energy and exploit it. The gear ratio of the VSA (fig.6.8 is brought to a minimum at 2.6s to maximise the acceleration of the end effector using both the motor and spring's power and then increases the gear ratio gradually until it

reaches an optimal point where increasing the gear ratio further would serve it badly in terms of final velocity.This is due to the position of the end effector where the gravitational force is acting against it's movement, in addition to the overdrive value of the gear ratio which requires a higher torque value to keep balance, so in other terms the limitation of power causes the lack of extra torque to keep increasing the gear ratio. The VSA reaches a maximum final velocity of 15.732 rad/s .

Criteria \ Device	VSA	SEA	Rigid actuator
Maximum distance (m)	2.68	1.9900	1.2745
Velocity at T (rad/s)	15.732	13.1178	9.7745
Time T (s)	2.5892	4.9981	3.3922

Table 6.1: Table showing different results for the same task done by different devices with variable time.

6.1.4 Discussion

After conducting the optimization on the three cases, the results for each experiment are summarized in the table 6.1.

The rigid actuator only uses the motor as a launch mechanism. The SEA achieved a significantly higher velocity and distance than the rigid actuator and finally the VSA achieved the highest of both devices. Both the SEA and VSA used the maximum motor power allowed towards the end of the task, but had achieved different outcomes(fig.6.7) and (fig.6.5). We can say the VSA used the power in a "smarter" way by manipulating it's stiffness to get the best out of the motor power, which is nothing but choosing the perfect combination of torque and velocity at the right time.

6.2 Energy consumption comparison

This simulation is intended to verify the energy efficiency of the different types of actuator. In this case the goal of the task will be to throw the object at the same distance. First, the trajectory will be optimized for the different actuators in order to get the fixed distance. Thanks to this optimization, it is ensured that the goal will be achieved with the minimal work required. The next step, the optimal trajectory will be used as a reference for the simulated system. The control scheme adopted will be the same described in Chapter 5.

6.2.1 Rigid actuator

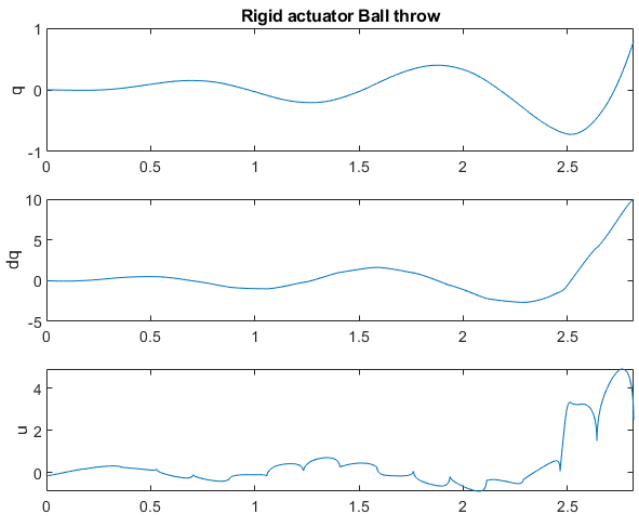

Figure 6.11: Simulated optimal trajectory for a rigid actuator with $\dot{\theta}(T) = 10$ rad/s and fixed throwing distance.

The rigid actuator tackles this task by trying to reach the maximum negative angle position (fig.6.11)by using minimal torque, and then applies enough torque to reach the desired final values.

6.2.2 SEA

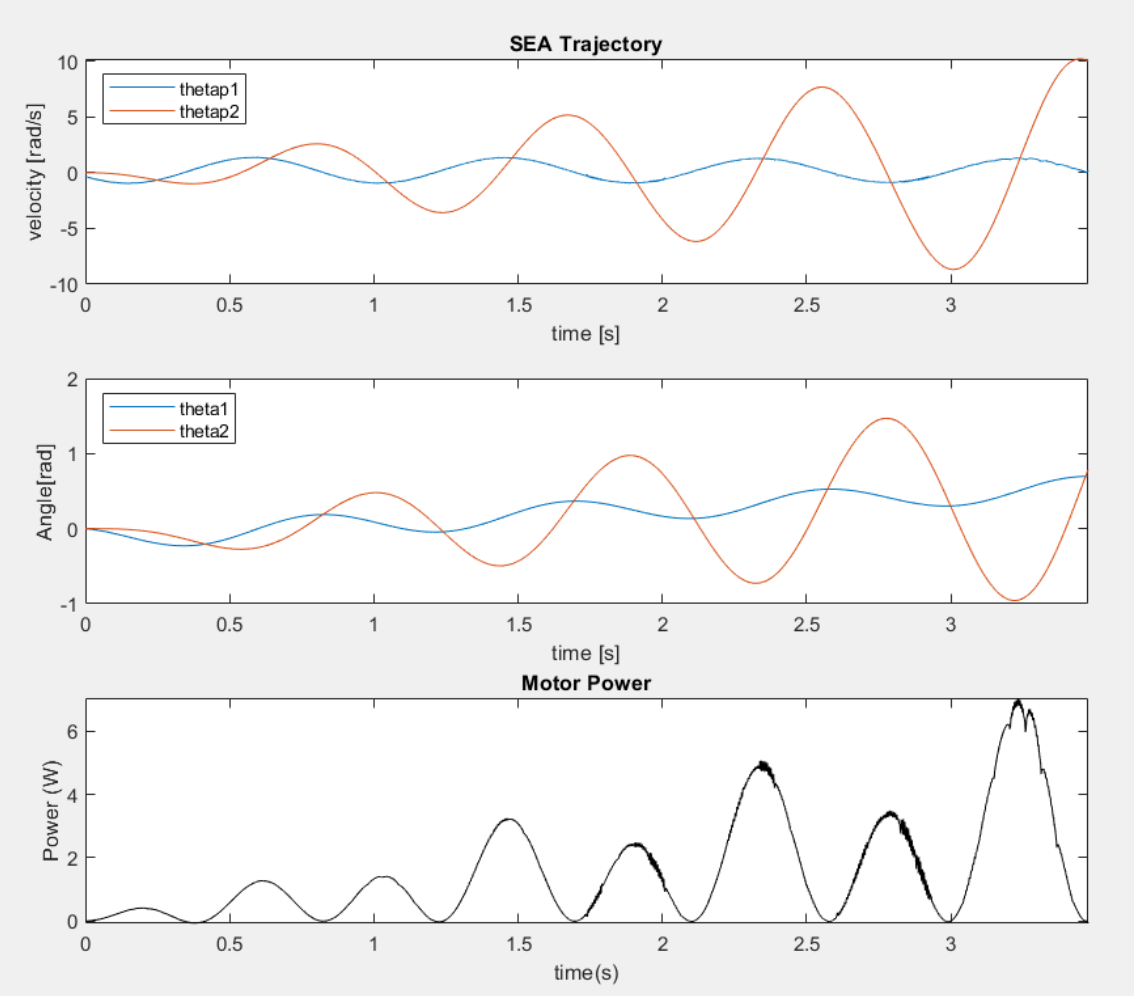

Figure 6.12: Simulated optimal trajectory for SEA with $\dot{\theta}_2 = 10$ rad/s and fixed thrown distance.

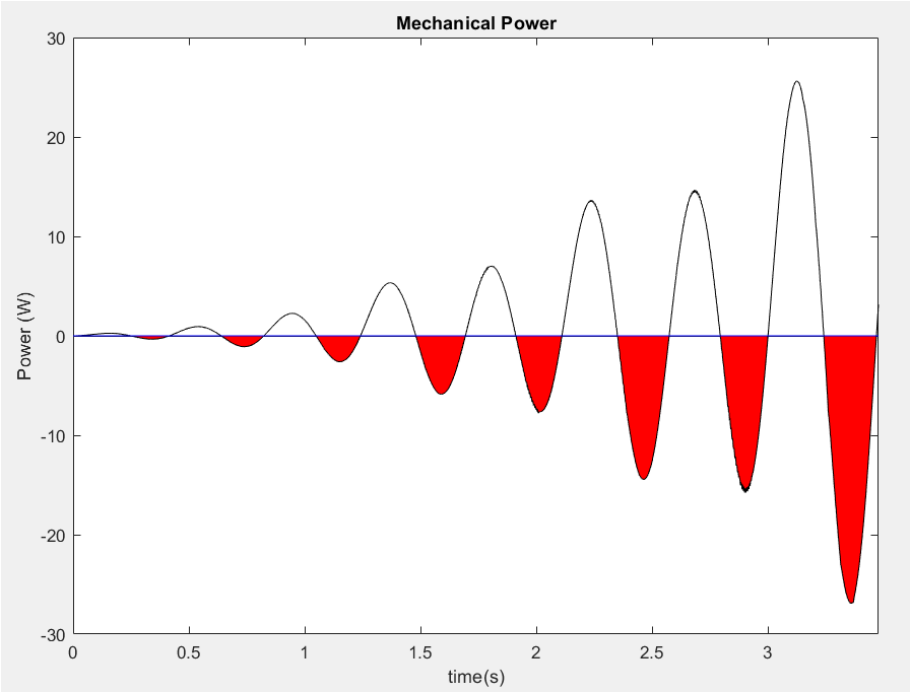

Figure 6.13: Simulated mechanical Power of SEA

The SEA charges the spring progressively in small amounts to keep the power at a minimum but at the same time increasing the spring energy storage at each oscillation until reaching the the energy in the spring enough to reach the desired final target.

6.2.3 VSA

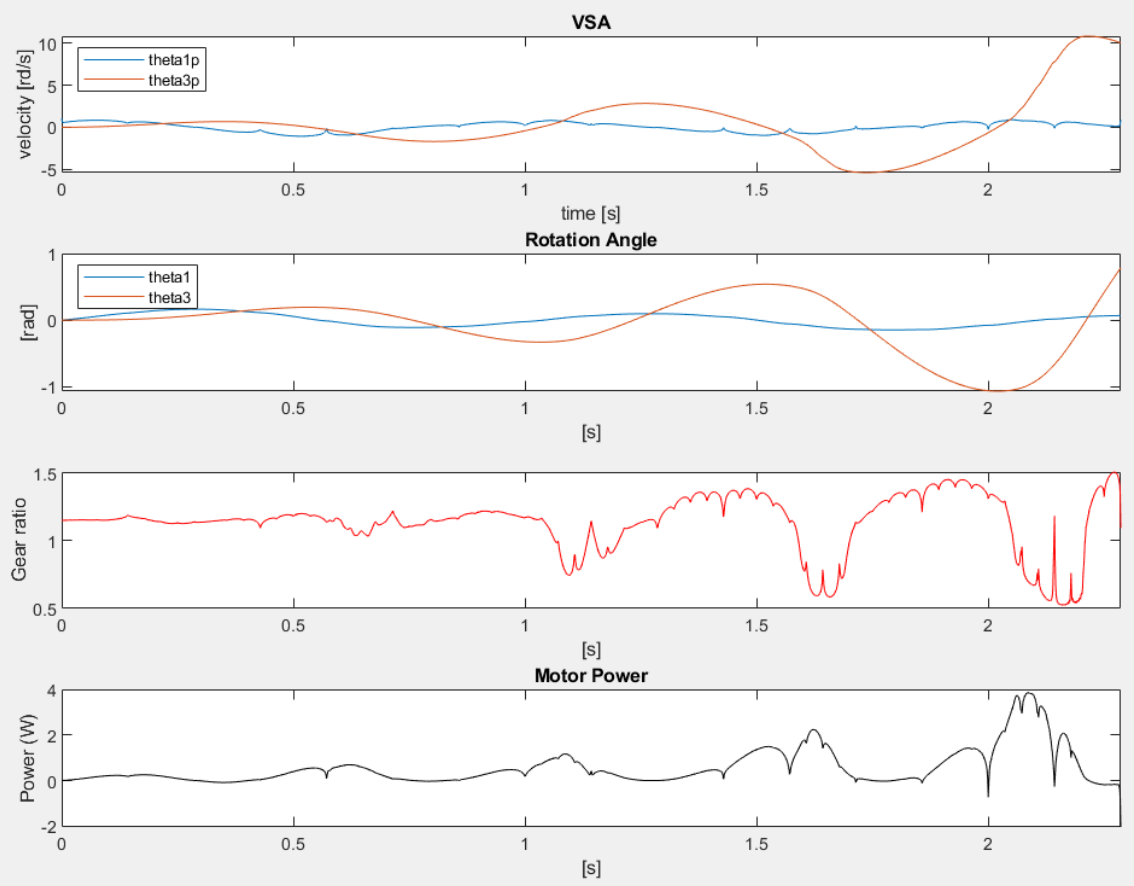

Figure 6.14: Simulated optimal trajectory for VSA with $\dot{\theta}_3(T) = 10$ rad/s and fixed thrown distance output.

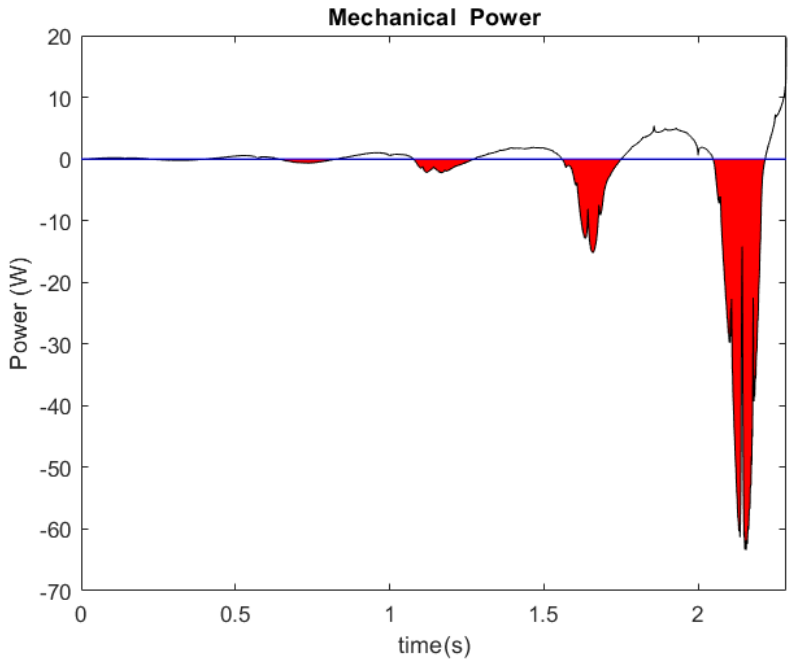

Figure 6.15: Mechanical Power of VSA

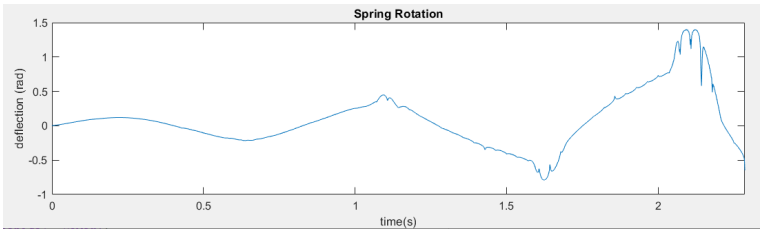

Figure 6.16: Spring deflection

Referring to (fig.6.14), (fig.6.15) and (fig.6.16). At 2s the spring is not fully rotated to the max deflection, and the end-effector reaches the highest negative position (high potential energy); the VSA takes advantage of this and charges the spring to reach it's high point. Then, to get the highest acceleration it keeps the gear ratio at it's lowest to get the maximum torque or instantaneous power from the spring (but for a shorter time) then it adjusts the gear ratio to get the desired final velocity without any power from the motor around the end.

6.2.4 Discussion

This Simulation has an objective to check the energy consumption for each device. In order to apply it in a fair way to all the three devices, the final results are set to

Criteria \ Device	VSA	SEA	Rigid actuator
Maximum distance (m)	1.3073	1.3073	1.3073
Velocity at T (rad/s)	10	10	10
Time T (s)	10	10	10
Energy consumption (J)	1.2904	5.3342	6.4858

Table 6.2: Table showing energy consumption of each device for the same distance thrown, final velocity.

be the same (throwing distance and final velocity), so the goal is not to maximize the throwing distance since they will all result in the same distance at the end of the task. Therefore the only difference is the approach each device takes to achieve the same result and the energy it needs to do so. So the objective of this task is not performance, but energy minimization, therefore the increase of the R factor (3.5), which is concerned with the running cost penalty, in other words, the priority of the cost function is highly focused on reaching the desired final results with as low energy consumption as possible.

The SEA, by charging the spring in small steps each period, has been able to achieve better efficiency than the rigid motor. However, it is still constrained by a single stiffness, which can limit the degree of freedom it can use the energy stored in its compliant element. In this specific task, the VSA strategy was to use a minimal amount of power to charge the spring where the peak power used is 4W, and it was used mostly in form of torque to maximize the deflection of the spring. This action was done around a negative position (-1 rad) of the end effector at 2s (fig.6.14), which is the last ascent of the end effector before release. What the VSA did was to maximize acceleration at the beginning of the ascent 2.25s and then stop the power flow from the motor, which was enough to let it reach the demanded final target. The VSA shows promising results since it can take advantage of storing the energy inside the spring and releasing it in different ways, it could be released in terms of very high instantaneous power (increased the stiffness) or released at a longer period of time with a lower power intensity (decreased stiffness), this option allows it to manage the stored power to be used at an optimum. The same goes for storing the energy, which in other words can be received in a high power intensity or received in a lower value but for a longer period of time. One example is impact, if we have a rigid body that receives an impact, the instantaneous power would be very high.But if for the VSA it can reduce the impact by varying the stiffness throughout the period of the impact by starting with a low stiffness and increasing it gradually to prevent extensive stress on the relative object. This device under

test shows much higher mechanical performance than it's contenders, but the gains acquired through these simulations are better than the ones that could be achieved in the real experiment, even though we have already considered the efficiency factor of the CVT, the friction elements have not been taken into consideration, which can only be acquired by testing the physical equipment. However, the concept is very similar to the real application, the major difference will be that the available output torque will be lower by a certain fraction after we account for the friction factors.

In this thesis, we have demonstrated the advantages to have a compliant element that has the ability to change it's characteristics in highly dynamic robotic application, in our case an explosive movement that is highly applicable in robotics where the robot has to undergo tasks that involve jumping, throwing objects or in general, to have a high amount of power in its disposal. We have also showed the importance of an optimal control that satisfies the constraints required by the application whether it was a movement restriction or a performance behaviour depending on the mechanics and dynamics of the device under study. We have also showed the ability of using a VSA in underpowered devices to achieve targets out of the device's dynamic range.

For future works, the goal will be to construct the mechanical device and extract the damping coefficient from the major components to get a model as close as possible to the real model and of course after doing so we would like to implement this prototype and validate the results obtained from the simulations.

List of Figures

List of Tables

Bibliography

[1] https://blog.universal-robots.com/how-service-robots-are-delivering-hope-and-helping-patients-rehabilitate

[2] https://builtin.com/robotics

[3] https://www.robotics.org/joseph-engelberger/unimate.cfm

[4] Modeling and Identification of an Industrial Robot for Machining Applications

[5] Dummy Crash-Tests for the Evaluation of RigidHuman-Robot Impacts Sami Haddadin, Alin Albu-Schaffer, Gerd Hirzinger

[6] https://clr.es/blog/en/electrical-actuators-robotics/

[7] https://nsmb.com/forum/forum/gear-4/topic/nuvinci–n360-cvt–hub–9894/

[8] Hugh Durrant-Whyte; Nicholas Roy; Pieter Abbeel, "Exploiting Variable Stiffness in Explosive Movement Tasks," in Robotics: Science and Systems VII , MITP, 2012, pp.25-32

[9] Variable impedance actuators: A review
B.Vanderborghtf A.Albu–Schaeffera A.Bicchibe E.Burdetd D.G.Caldwelle R.Carlonic M.Catalanobe O.Eibergera W.Friedla G.Ganeshd M.Garabinib M.GrebensteinaG.Griolib S.Haddadina H.Hoppnera A.Jafarie M.Laffranchie D.Lefeberf F.Petita S.Stramigiolic N.Tsagarakise M.Van Dammef R.Van Hamf L.C.Visserc S.Wolfa

[10] Grioli, G., Wolf, S., Garabini, M., Catalano, M., Burdet, E., Caldwell, D., Bicchi, A. (2015). Variable stiffness actuators: The user's point of view. The International Journal of Robotics Research, 34(6), 727–743.

[11] https://www.autodesk.com/redshift/history-of-industrial-robots/

[12] http://webhome.auburn.edu/ vestmon/robotics.html

[13] B. Matthias, S. Oberer-Treitz, H. Staab, E. Schuller and S. Peldschus, "Injury Risk Quantification for Industrial Robots in Collaborative Operation with Humans," ISR 2010 (41st International Symposium on Robotics) and ROBOTIK 2010 (6th German Conference on Robotics), Munich, Germany, 2010, pp. 1-6.

[14] By Daimler und benz Stiftung - Daimler und Benz Stiftung, CC BY-SA 3.0 de, https://commons.wikimedia.org/w/index.php?curid=322619

[15] Komati, Bilal & Pac, Muhammed & Ranatunga, Isura & clevy, cedric & Popa, Dan & Lutz, Philippe. (2013). Explicit Force Control vs Impedance Control for Micromanipulation. Proceedings of the ASME Design Engineering Technical Conference. 1. 10.1115/DETC2013-13067.

[16] Villani L., De Schutter J. (2008) Force Control. In: Siciliano B., Khatib O. (eds) Springer Handbook of Robotics. Springer, Berlin, Heidelberg

[17] Robot Force Control: An Introduction - Robotiq's Blog https://blog.robotiq.com/bid/53553/Robot-Force-Control-An-Introduction

[18] N. Hogan, "Impedance Control: An Approach to Manipulation," 1984 American Control Conference, San Diego, CA, USA, 1984, pp. 304-313.

[19] Sami Haddadin, Tim Laue, Udo Frese, Sebastian Wolf, Alin Albu–Schaffer, Gerd Hirzinger, Kick it with elasticity: Safety and performance in human–robot soccer, Robotics and Autonomous Systems, Volume 57, Issue 8, 2009, Pages 761–775, ISSN 0921–8890, Sami Haddadin, Tim Laue b, Udo Frese b, Sebastian Wolfa, Alin Albu- Schaffer a, Gerd Hirzinger a

[20] M. Mosadeghzad, G. A. Medrano-Cerda, J. A. Saglia, N. G. Tsagarakis and D. G. Caldwell, "Comparison of various active impedance control approaches, modeling, implementation, passivity, stability and trade-offs," 2012 IEEE/ASME International Conference on Advanced Intelligent Mechatronics (AIM), Kachsiung, 2012, pp. 342-348.

[21] S. Eppinger and W. Seering, "Understanding bandwidth limitations in robot force control," Proceedings. 1987 IEEE International Conference on Robotics and Automation, Raleigh, NC, USA, 1987, pp. 904-909.

[22] S. Katsura, Y. Matsumoto and K. Ohnishi, "Analysis and experimental validation of force bandwidth for force control," in IEEE Transactions on Industrial Electronics, vol. 53, no. 3, pp. 922-928, June 2006.

[23] Y. F. Li and X. B. Chen, "On the dynamic behavior of a force/torque sensor for robots," in IEEE Transactions on Instrumentation and Measurement, vol. 47, no. 1, pp. 304-308, Feb. 1998.

[24] Series Elastic Actuator Gill A. Pratt and Matthew M. Williamson MIT Artificial Intelligence Laboratory and Laboratory for Computer Science

[25] Alexander, R. McNeill, "Elastic Mechanisms in Animal Movement", Cambridge University Press, 1988.

[26] Basafa, Ehsan & Salarieh, Hassan & Alasty, Aria. (2007). Modeling and Control of Nonlinear Series Elastic Actuator. 10.1115/DETC2007-34997.

[27] I. Thorson and D. Caldwell, "A nonlinear series elastic actuator for highly dynamic motions," 2011 IEEE/RSJ International Conference on Intelligent Robots and Systems, San Francisco, CA, 2011, pp. 390-394.

[28] Jung-Jun Park, Byeong-Sang Kim, Jae-Bok Song, Hong-Seok Kim, Safe link mechanism based on nonlinear stiffness for collision safety, Mechanism and Machine Theory, Volume 43, Issue 10, 2008, Pages 1332-1348, ISSN 0094-114X,

[29] Visser L, Carloni R and Stramigioli S (2010) Energy efficient control of robots with variable stiffness actuators. In: Proceedings of the IFAC international symposium on nonlinear control systems.

[30] Visser LC, Stramigioli S and Bicchi A (2011) Embodying desired behavior in variable stiffness actuators. In: 18th IFAC world congress. IFAC. Wimboeck T, Ott C and

[31] M. Malosio, M. Caimmi, G. Legnani and L. M. Tosatti, "LINarm: a low-cost variable stiffness device for upper-limb rehabilitation," 2014 IEEE/RSJ International Conference on Intelligent Robots and Systems, Chicago, IL, 2014, pp. 3598-3603.

[32] Tsagarakis, Nikos & Sardellitti, Irene & Caldwell, D.G.. (2011). A new variable stiffness actuator (CompAct-VSA): Design and modelling. Proceedings of the ... IEEE/RSJ International Conference on Intelligent Robots and Systems. IEEE/RSJ International Conference on Intelligent Robots and Systems. 378-383. 10.1109/IROS.2011.6095006.

[33] TESTING OF A SPRING WITH CONTROLLABLE STIFFNESS
Waldemar RACZKA

[34] S. Kawamura et al., "Development of passive elements with variable mechanical impedance for wearable robots," Proceedings 2002 IEEE International Conference on Robotics and Automation (Cat. No.02CH37292), Washington, DC, USA, 2002, pp. 248-253 vol.1.

[35] Osamu Tabata, Satoshi Konishi, Pierre Cusin, Yuichi Ito, Fumie Kawai, Shinichi Hirai, Sadao Kawamura, Micro fabricated tunable bending stiffness devices, Sensors and Actuators A: Physical, Volume 89, Issues 1–2, 2001, Pages 119-123, ISSN 0924-4247, https://doi.org/10.1016/S0924-4247(00)00538-0.

[36] T. Morita and S. Sugano, "Design and development of a new robot joint using a mechanical impedance adjuster," Proceedings of 1995 IEEE International Conference on Robotics and Automation, Nagoya, Japan, 1995, pp. 2469-2475 vol.3.

[37] M. Garabini, A. Passaglia, F. Belo, P. Salaris and A. Bicchi, "Optimality principles in variable stiffness control: The VSA hammer," 2011 IEEE/RSJ International Conference on Intelligent Robots and Systems, San Francisco, CA, 2011, pp. 3770-3775.

[38] Vanderborght, B.; Tsagarakis, N.; van Ham, R.; Thorson, I.; Caldwell, D. MACCEPA 2.0: Compliant actuator used for energy efficient hopping robot chobino 1D. Autonom. Rob. 2011,31, 55–65.

[39] Huang, Y.; Vanderborght, B.; van Ham, R.; Wang, Q.; van Damme, M.; Guangming, X.; Lefeber, D. Step length and velocity control of dynamic bipedal walking robot with adaptable compliant joints. IEEE/ASME Trans. Mechatron. 2013,18, 598–611

[40] Mao, Y.; Wang, J.; Jia, P.; Li, S.; Qiu, Z.; Zhang, L.; Han, Z. A reinforcement learning based dynamic walking control. In Proceedings of the IEEE International Conference on Robotics and Automation, 10-14 April 2007; pp. 3609–3614.

[41] Stramigioli, Stefano & Oort, Gijs & Dertien, Edwin. (2008). A concept for a new Energy Efficient Actuator. 671 - 675. 10.1109/AIM.2008.4601740.

[42] https://wikicars.org/en/Continuously_Variable_Transmission

[43] Nilabh Srivastava, Imtiaz Haque,
A review on belt and chain continuously variable transmissions (CVT): Dynamics and control,
Mechanism and Machine Theory,
Volume 44, Issue 1,
2009,
Pages 19-41,
ISSN 0094-114X

[44] https://www.nsk.com/products/automotive/drive/hcvt/index.html

[45] Ms. Tanvi Dilip Challirwar (2019). Continuously Variable Transmission (CVT). International Journal of Engineering Trends and Technology, 67(3), 62-65

[46] https://en.wikipedia.org/wiki/Continuously_variable_transmission

[47] Carter, Jeremy et al. "Use of a Continuously Variable Transmission to Optimize Performance and Efficiency of Two-Wheeled Light Electric Vehicles (LEV)." (2009).

[48] Sami Haddadin, Michael Weis, Sebastian Wolf, Alin Albu–Schaffer, Optimal Control for Maximizing Link Velocity of Robotic Variable Stiffness Joints, IFAC Proceedings Volumes, Volume 44, Issue 1, 2011, Pages 6863-6871, ISSN 1474-6670, ISBN 9783902661937

[49] An Introduction to Trajectory Optimization
Matthew Kelly

[50] Development of Multiple-Phase Trajectory Planner Using Legendre-Gauss-Radau Collocation Methods

[51] https://www.mathworks.com/discovery/nonlinear-programming.html

[52] W. L. Nelson. Physical principles for economies of skilled movements. Biological Cybernetics, 46(2):135–147, 1983.

[53] Jacques Vlassenbroeck, A chebyshev polynomial method for optimal control with state constraints, Automatica, Volume 24, Issue 4, 1988, Pages 499-506, ISSN 0005-1098,

[54] Smithson, R., Miller, D., and Allen, D., "Scalability for an Alternative Rolling Traction CVT," SAE Technical Paper 2004-01-0355, 2004

[55] Vallery, Heike Ekkelenkamp, Ralf Kooij, Herman Buss, Martin. (2007). Passive and accurate torque control of series elastic actuators. 2007 IEEE/RSJ International Conference on Intelligent Robots and Systems. 3534-3538. 10.1109/IROS.2007.4399172

[56] Stiffness Isn't Everything Gill A. Pratt, Matthew M. Williamson, Peter Dillworth, Jerry Pratt, Karsten Ulland, Anne Wright MIT Artificial Intelligence Laboratory and Laboratory for Computer Science

[57] Wyeth, Gordon (2006) Control issues for velocity sourced series elastic actuators. In MacDonald, B (Ed.) Proceedings of the 2006 Australasian Conference on Robotics and Automation. Australian Robotics and Automation Association, Australia, pp. 1–6.

[58] http://www.gysin.com/en/products/gears/